4794 J. Med. Chem. 2009, 52, 4794–4809
DOI: 10.1021/jm900357y

Journal of Medicinal Chemistry Article

Combining Hit Identification Strategies: Fragment-Based and in Silico Approaches to Orally Active 2-Aminothieno[2,3-*d*]pyrimidine Inhibitors of the Hsp90 Molecular Chaperone

Paul A. Brough,*[,†] Xavier Barril,[†] Jenifer Borgognoni,[†] Patrick Chene,[§] Nicholas G. M. Davies,[†] Ben Davis,[†] Martin J. Drysdale,[†] Brian Dymock,[†] Suzanne A. Eccles,[‡] Carlos Garcia-Echeverria,[§] Christophe Fromont,[†] Angela Hayes,[‡] Roderick E. Hubbard,[†] Allan M. Jordan,[†] Michael Rugaard Jensen,[§] Andrew Massey,[†] Angela Merrett,[†] Antony Padfield,[†] Rachel Parsons,[†] Thomas Radimerski,[§] Florence I. Raynaud,[‡] Alan Robertson,[†] Stephen D. Roughley,[†] Joseph Schoepfer,[§] Heather Simmonite,[†] Swee Y. Sharp,[‡] Allan Surgenor,[†] Melanie Valenti,[‡] Steven Walls,[†] Paul Webb,[†] Mike Wood,[†] Paul Workman,[‡] and Lisa Wright[†]

[†]*Vernalis Ltd., Granta Park, Great Abington, Cambridge CB21 6GB, U.K.,* [‡]*Cancer Research UK Centre for Cancer Therapeutics, The Institute of Cancer Research, Haddow Laboratories, Sutton, Surrey SM2 5NG, U.K., and* [§]*Novartis Institutes for Biomedical Research, Novartis Pharma AG, CH-4002 Basel, Switzerland*

Received March 21, 2009

Inhibitors of the Hsp90 molecular chaperone are showing considerable promise as potential molecular therapeutic agents for the treatment of cancer. Here we describe novel 2-aminothieno[2,3-*d*]pyrimidine ATP competitive Hsp90 inhibitors, which were designed by combining structural elements of distinct low affinity hits generated from fragment-based and in silico screening exercises in concert with structural information from X-ray protein crystallography. Examples from this series have high affinity (IC_{50} = 50−100 nM) for Hsp90 as measured in a fluorescence polarization (FP) competitive binding assay and are active in human cancer cell lines where they inhibit cell proliferation and exhibit a characteristic profile of depletion of oncogenic proteins and concomitant elevation of Hsp72. Several examples (**34a**, **34d** and **34i**) caused tumor growth regression at well tolerated doses when administered orally in a human BT474 human breast cancer xenograft model.

Introduction

Heat shock protein 90 (Hsp90) is an important member of a class of proteins known as molecular chaperones. These chaperone proteins play a critical role in the conformational maturation, stability, and function of other "client" protein substrates within the cell.[1] The mechanism of action of Hsp90 is complex, involving homodimerization and binding to substrates, cochaperones, and other accessory proteins operating in a chaperone cycle.[2] This cycle is driven by the binding of ATP to Hsp90, hydrolysis to ADP, and subsequent ATP/ADP exchange, which enables the multimeric complexes within the conformational cycle to facilitate protein loading, activation, and release.[3−5]

There are over 100 client proteins of Hsp90 identified to date,[6] many of which are involved in signal transduction, cell cycle regulation, and apoptosis, including kinases, transcription factors, and hormone receptors.[7−10] The dysregulation of pathways involving these proteins is commonly associated with cancer pathology and Hsp90 thus plays a key role in assisting survival, proliferation, invasion, metastasis, and angiogenesis. Inhibition of Hsp90 function is therefore considered as a major therapeutic target, as it constitutes a combinatorial attack on these hallmark traits of cancer,[11] with the potential for broad spectrum activity and reduced liability for acquired drug resistance as a consequence of the ability to interfere with multiple oncogenic pathways.[12]

Pioneering studies with natural product inhibitors of Hsp90 function such as geldanamycin[13−15] (GM) and radicicol[16,17] (RD; Figure 1, **1a** and **2**) provided valuable characterization and showed that both GM and RD are able to inhibit Hsp90 function by binding to the ATP binding pocket in the N-terminal domain of Hsp90.[18] The subsequent arrest of the Hsp90 chaperone cycle causes client proteins to be degraded by the ubiquitin−proteasome pathway, leading to cell cycle arrest and apoptosis in cancer cells.[19] Further validation and proof of principle that Hsp90 is a promising anticancer drug has come from animal models and clinical studies with the GM analogue 17-allylamino-17-demethoxygeldanamycin (17-AAG; Figure 1; **1b**).[20] This first-in-class Hsp90 inhibitor has demonstrated evidence of target modulation and indications of clinical activity in melanoma, prostate, renal, multiple myeloma, and trastuzumab-refractory breast cancer.[21−24] Additional clinical trials have been initiated with 17-AAG used as a single agent and in drug combinations in various cancer types. The prevalence of a high affinity form of Hsp90 in tumor cells,[25] the "addiction" of cancer cells to oncogenic client proteins, and the greater dependency upon Hsp90 of these clients (especially their activated mutated forms)[26] have been proposed as rationales for the remarkable selectivity of Hsp90 inhibitors for cancer versus normal cells.[27]

However, despite the good activity in preclinical models and the clinical progression of 17-AAG, this compound has several potential limitations including poor solubility, necessitating complex formulations, limited bioavailability, hepatotoxicity, and extensive metabolism by polymorphic

*To whom correspondence should be addressed. Phone 44 (0)1223 895372. Fax: 44 (0)1223 895556. E-mail: p.brough@vernalis.com.

 Published on Web 07/17/2009

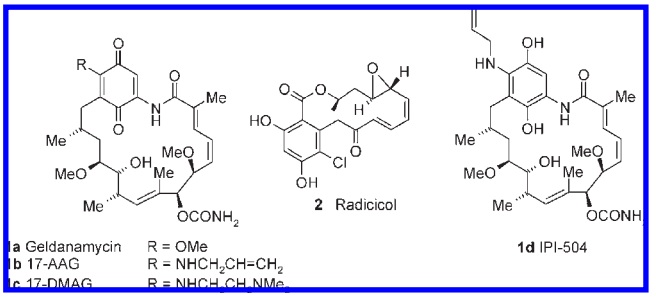

Figure 1. Natural product derived Hsp90 inhibitors.

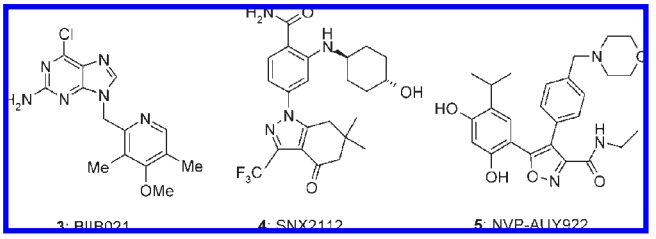

Figure 2. Purine, benzamide, and resorcinol scaffold Hsp90 inhibitors progressed to phase I trials.

enzymes.[28−30] In particular, low level expression or mutation of the oxidoreductase NQO1, which catalyzes reduction of the benzoquinone moiety, has been shown to give rise to intrinsic and acquired resistance to 17-AAG.[31] Some of these issues have been addressed with the development of the water-soluble ansamycin 17-dimethylamino-ethylamino-17-demethoxygeldanamycin (17-DMAG; Figure 1; **1c**),[32] which was in phase I/Ib clinical trials, and the hydroquinone pro-drug of 17-AAG (IPI-504; Figure 1; **1d**),[33,34] which is reported to be in phase I/II. A proprietary formulation of 17-AAG (KOS-953)[35] has advanced to phase III in combination with bortezomib (www.clinicaltrials.gov). However, the above issues and the inherent chemical complexity of the ansamycin inhibitors have led to significant efforts to identify novel small-molecule inhibitors of Hsp90 and this arena of research has been extensively reviewed.[29,36−47] The most advanced small molecule inhibitors described to date include purine,[48,49] benzamide,[50] and resorcinol[51,52] scaffold inhibitors as exemplified by compounds **3**−**5**, respectively (Figure 2). These compounds are reportedly in phase I clinical trials for cancer.[53] We recently reported on the structure-based drug design program that led to the identification of the highly potent resorcinol inhibitor **5** (NVP-AUY922/VER-52296; Figure 2).[51] To deliver an orally bioavailable inhibitor back up compound, we felt it appropriate to identify a novel ATP competitive small molecule inhibitor with a distinct chemotype. Herein we report on the combination of hit identification strategies and the structure-based medicinal chemistry program that led to the identification of a new class of 2-aminothieno[2,3-*d*]pyrimidine Hsp90 inhibitors with oral efficacy in animal models of cancer.

Hit Identification

Finding novel compounds as starting points for optimization is a major challenge in drug discovery research. Fragment-based methods[54−59] have emerged in the past 10 years as an effective way to sample chemical diversity with a limited number of low molecular weight compounds. The structures of the fragment binding to the protein can then be used to design new compounds with increased affinity, specificity and

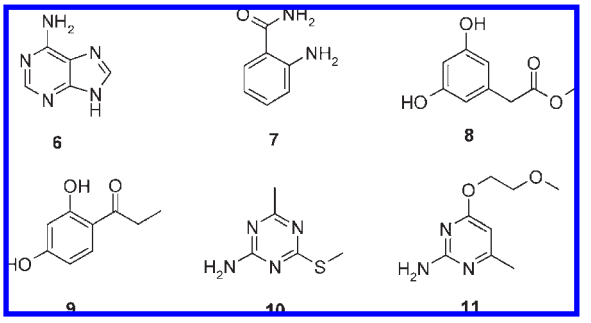

Figure 3. Structures of Hsp90α ATP site binding fragments identified by 1D NMR experiments.

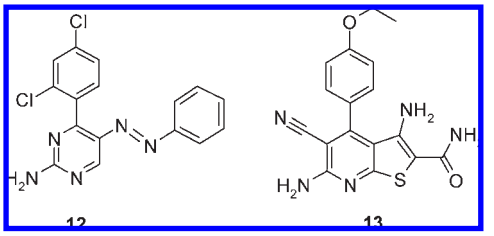

Figure 4. Structures of Hsp90 ligands identified by virtual screening.

novelty. The approach we applied has been previously described[60] and included (i) the design of a fragment library, (ii) identification of fragments that bound competitively to Hsp90 by ligand-based NMR techniques, and (iii) rationalization of the fragment binding mode in the ATP binding site of Hsp90 by protein X-ray crystallography. This structural information was then used to evolve the fragments to hits, either by growing the fragment or by combining structural features from a number of compounds. Fragments bind to protein targets with relatively weak affinity, and for this reason, screening had to be conducted with the potential ligands at high concentrations. It was therefore important to devise a strategy that identified specific binding of fragments to the targeted site of the protein and that could exclude nonspecific or distal binding.

The strategy employed was to identify fragments that bound to the enzyme and that were then displaced by a competitor molecule, in this case the purine scaffold inhibitor PU3,[61] in a manner analogous to a standard biochemical competition assay. A wide variety of NMR methods have been proposed to monitor ligand binding.[62] We have found that a combination of three widely used approaches (saturation transfer difference (STD),[63] water-LOGSY,[64] and T2 relaxation filtered 1D[65]) gave a substantially more reliable experimental output than the use of any single technique and added little to the duration of either the data acquisition or analysis stages of the study. The designed fragment library[66] was screened against N-terminal domain human Hsp90α by combining 10−12 compounds per tube. This number of compounds was found to be optimal before resonance overlap became an experimental issue with respect to spectral analysis. Spectra were recorded in presence and absence of the ATP competitive ligand PU3,[61] and compounds that bound to Hsp90 were categorized as "Class 1" hits[60] if the expected changes on addition of the competitor ligand were seen with all three NMR experiments. The overall hit rate from an NMR screen of 1351 fragments was 6.1% (82 compounds), of which 59 compounds bound in all three

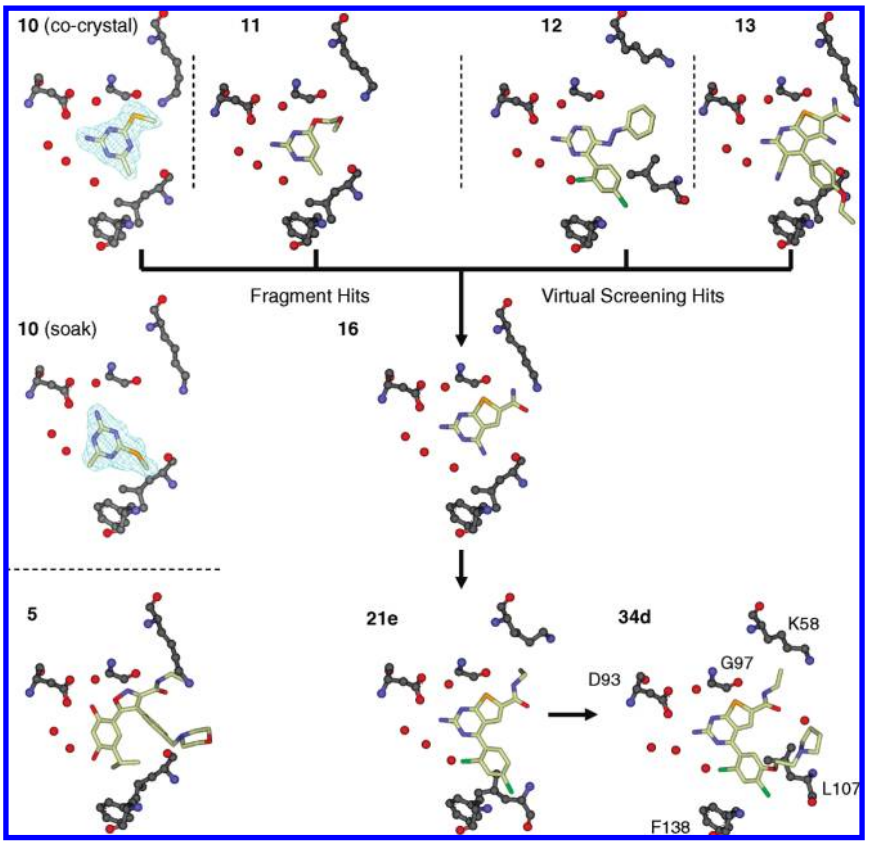

Figure 5. Detail of the X-ray crystal structures of N-terminal-Hsp90α in complex with a series of fragments and ligands, highlighting key protein amino acids and water molecules (red spheres).[80] The structures were overlapped on the main chains of residues T109-D102 and T115-G215, which omit the flexible helix and N and C termini. The rmsd was between 0.22 and 0.40 Å across the data set. Protein carbon atoms in gray (bond types not shown), oxygen in red, nitrogen in blue, chlorine in green, sulfur in yellow. Electron density for **10** is $2F_o - F_c$ map, contoured at 3σ. All structures are from ligand soaks except where stated.

Scheme 1. Synthesis of Close Analogues of the Fragment Hits **10** and **11**[a]

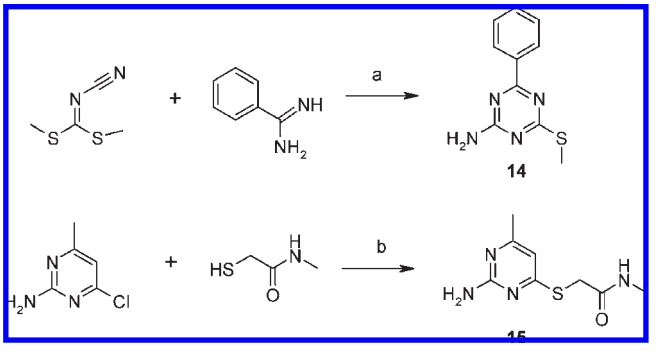

[a] Reagents and conditions: (a) diisopropylamine, EtOH, 65 °C, 3.5 h, 30%. (b) MeOH, Et_3N, microwave, 120 °C, 10 min, 14%.

Scheme 2. Synthesis of the 2,4-Diaminothieno[2,3-*d*]pyrimidine Scaffold[a]

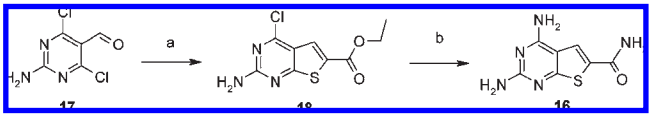

[a] Reagents and conditions: (a) ethyl-2-mercaptoacetate, K_2CO_3, MeCN, 85 °C, 5 h, 82%. (b) aq NH_3, microwave 130 °C, 15 min, 22%.

experiments; 21 compounds bound in two of the experiments, and 2 compounds bound in only one experiment. Selected

Scheme 3. Synthesis of 4-Aryl 2-Aminothieno[2,3-*d*]pyrimidines **21a**−**21e**[a]

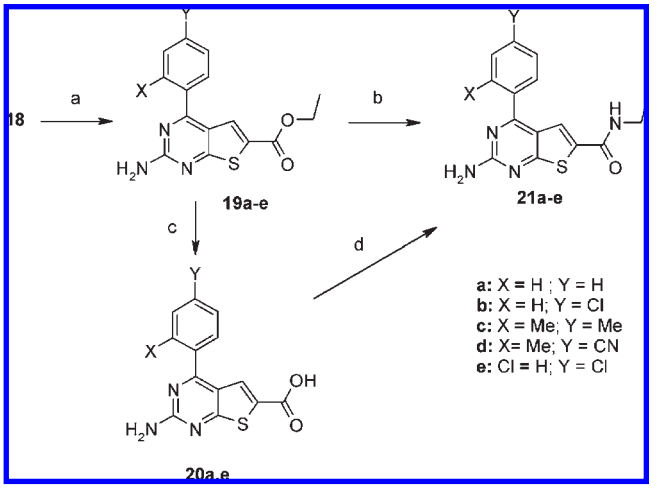

[a] Reagents and conditions: (a) 2X,4Y-phenylboronic acid, DMF, H_2O, $Pd(PPh_3)_2Cl_2$, $NaHCO_3$, Δ. (b) $EtNH_2$, MeOH, 85 °C (sealed tube), 18 h. (c) NaOH, H_2O, EtOH, Δ. (d) HATU, diisopropylamine, $EtNH_2 \cdot HCl$, DMF, 100 °C.

class 1 hits are shown in Figure 3 (compounds **6**−**11**). A significant number of noncompetitive compounds were identified from the NMR screening (158 in total). These compounds bound to Hsp90 but were not displaced by PU3 in the competition step and were thus not classed as hits and not

Scheme 4. Synthesis of 5′-Alkyloxy-2-aminothieno[2,3-*d*]pyrimidine Hsp90 Inhibitors **34a**−**i**[a]

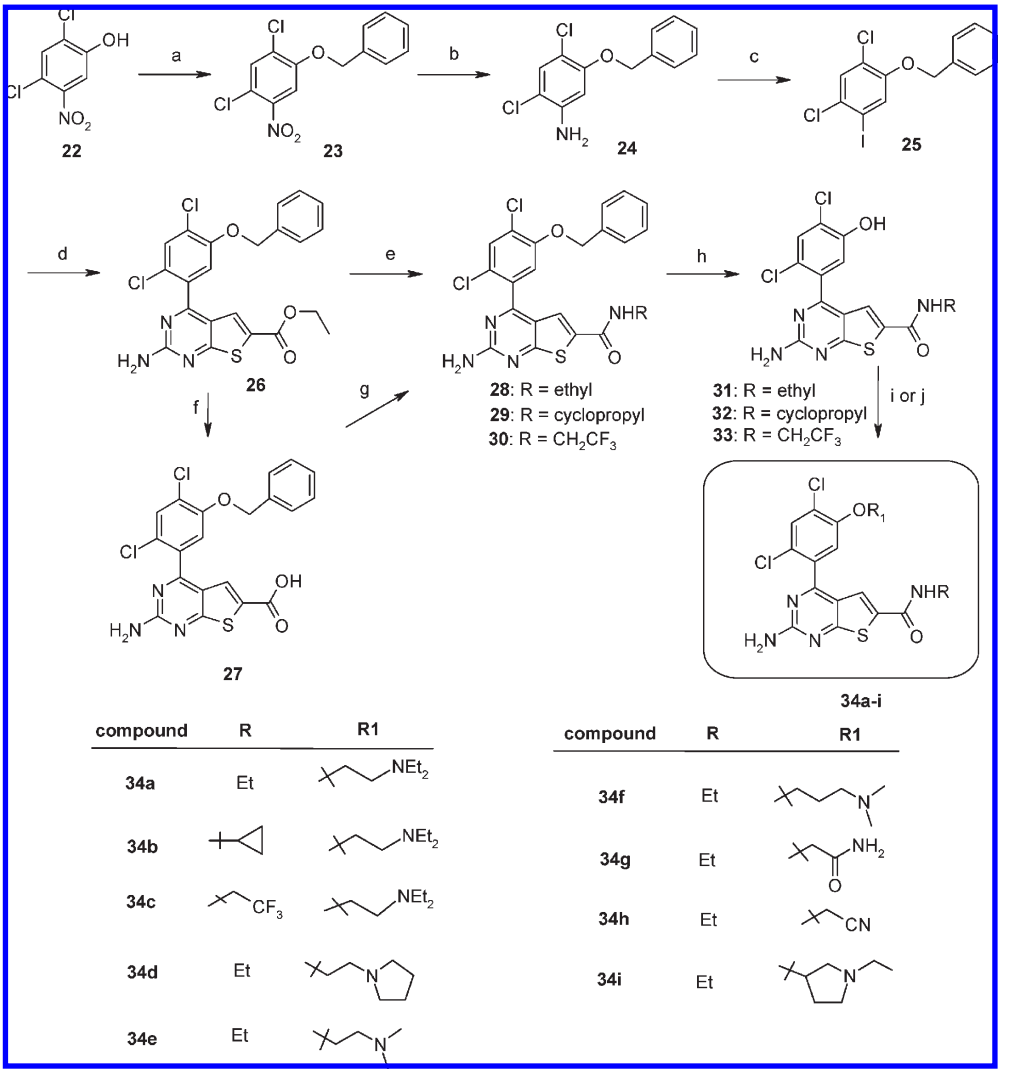

[a] Reagents and conditions: (a) BnBr, K_2CO_3, MeCN, Δ, 18 h, 96%. (b) Iron powder, AcOH, H_2O, 85 °C, 1.5 h, 96%. (c) (i) $NaNO_2$, HCl, H_2O, AcOH, 0 to 5 °C, 30 min; (ii) I_2, KI, H_2O, rt,1.5 h, 90%. (d) (i) KOAc, bis(pinacolato)diboron, $Pd(OAc)_2$, DMF, 90 °C, 18 h; (ii) **18**, K_3PO_4, 1,4-dioxane, $Pd(PPh_3)_2Cl_2$, 100 °C, 3 h, 45%. (e) $EtNH_2$, MeOH, Δ, 18 h, 84%. (f) NaOH, H_2O, EtOH, D, 50 min, quant. (g) HATU, RNH_2, DMF, diisopropylamine; 50 °C, 1 h. (h) BCl_3, CH_2Cl_2, −78 °C to rt, 3 h, 87%. (i) R_1Br/Cl, Cs_2CO_3, DMF, 100−140 °C, 1−2 h. (j) R_1OH, DIAD, PPh_3, THF, rt, 4 h.

Scheme 5. Synthesis of Aminothieno[2,3-*d*]pyrimidine Hsp90 inhibitors **34j**−**m** via Reductive Amination[a]

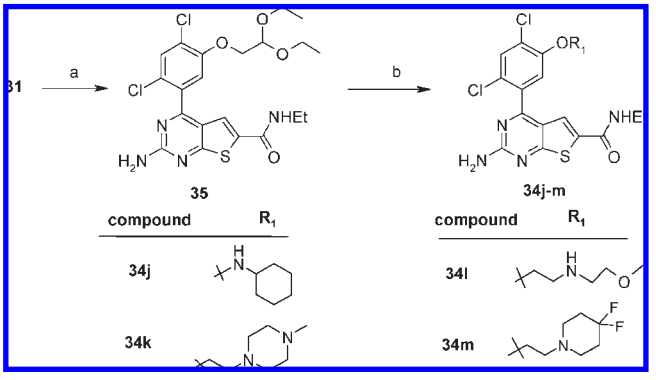

[a] Reagents and conditions: (a) 2-Bromoethylacetaldehyde diethyl acetal, Cs_2CO_3, DMF, 125 °C, 4 h, 71%. (b) (i) HCl (aq), THF, 48 h; (ii) amine, DCM, $NaB(OAc)_3H$, 1.5 h.

Table 1. Binding Affinities[a] for Hsp90 ATP Binding Site Measured by Fluorescence Polarization Assay for Selected Fragment and Virtual Screening Hits

compd no.	FP IC_{50} (μM)	compd no.	FP IC_{50} (μM)
6	>4000	**12**	1.56
7	>4000	**13**	0.90
8	490	**14**	20
9	570	**15**	535
10	350	**16**	1250
11	>4000		

[a] Values are reported as a mean of at least two independent determinations.

further characterized. X-ray crystallography using the N-terminal domain of human Hsp90α established the binding mode of compounds **6**−**11** and structurally related fragments. It was interesting to note that the purine (**6**), 2-amino benzamide (**7**), and resorcinol fragments (**8** and **9**, Figure 3) all contain structural motifs found in the inhibitors described in

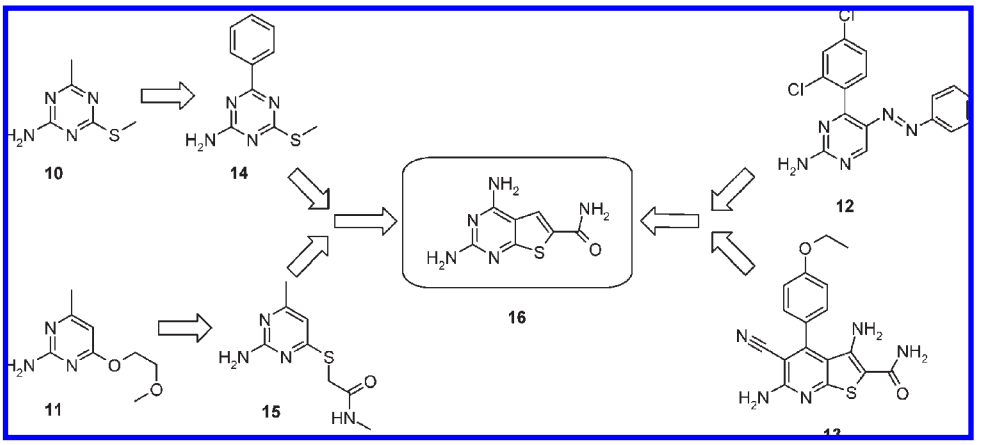

Figure 6. Combining fragment and virtual screening hits; evolution to the 2-aminothieno[2,3-*d*]pyrimidine scaffold.

Table 2. Binding Affinities[a] for Hsp90 ATP Binding Site Measured by Fluorescence Polarization Assay and Antiproliferation Potency (GI_{50})[b] in a Human HCT116 Colon Carcinoma Cell Line for Selected 2-Amino-4-aryl-thieno[2,3-*d*]pyrimidine Hsp90 Inhibitors

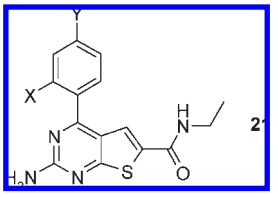

compd no.	X	Y	FP IC_{50} (μM)	GI_{50} (HCT116) (μM)
21a	H	H	5.7	14.3
21b	H	Cl	0.72	8.47
21c	Me	Me	0.34	4.24
21d	Me	CN	0.30	1.34
21e	Cl	Cl	0.23	0.82

[a] Values are reported as a mean of at least two independent determinations. [b] Antiproliferative potency as indicated by concentrations which lead to 50% growth inhibition (GI_{50}) in a SRB assay.

Figure 2. Another fragment-based approach to identifying Hsp90 ligands has been subsequently disclosed.[67] Elaboration of the initial fragment hits (which included a fragment linking strategy) led to the identification of high affinity Hsp90 ligands, although further biological characterization was not discussed. Recently, another group has reported on a fragment-based approach, which led to the identification of tetrahydrobenzopyrimidine Hsp90 inhibitors.[68]

We applied a parallel approach to hit identification, namely in silico (or virtual) screening. There has recently been increasing success in using molecular docking methods in the discovery of new chemical entities that bind to therapeutic target proteins, including Hsp90.[69,70] We utilized the proprietary docking software rDock and a previously described docking protocol[69,71] in an effort to identify novel Hsp90 ligands. The shape and size of the ATP binding site is altered upon binding of PU3 as a consequence of a flexible loop between residues 104 to 111.[72] Therefore the structure of both open and helical forms (PDB codes 1YET and 1UY6) were used in the docking, and in addition, three highly conserved water molecules in the region of the D93 residue were treated as part of the receptor. A virtual library of 700000 compounds was selected from the 3.5 million commercially available compounds in our proprietary catalogue rCat.[73] The output from the screen was further filtered to identify 719 commercially available compounds, which were obtained and screened in a fluorescence polarization (FP) assay,[74] which measured directly competitive binding to the N-terminal ATP binding site. This exercise identified a number of hits including **12** and **13** (Figure 4). The binding affinity of these hits and the fragment derived hits disclosed in Figure 3 are shown in Table 1. These data demonstrated a number of hits with weak to moderate affinity for the Hsp90 ATP site. In addition to these binding data, X-ray crystallography provided structural information (Figure 5) to guide further optimization. The challenge was to combine the structure−activity relationships (SAR) and X-ray crystallographic data relating to these hits (and other Hsp90 inhibitors) to enable the rapid progression to tractable leads and subsequent lead optimization.

Chemistry

The 1,3,5 triazine **14** was prepared as outlined in Scheme 1 by condensation of benzamidine hydrochloride with dimethyl cyanodithioiminocarbonate by a modification of a method previously described.[75] Pyrimidine **15** was prepared by the microwave mediated reaction of the commercially available 2-amino-4-chloro-6-methylpyrimidine with 2-mercapto-*N*-methyl acetamide. The thienopyrimidine scaffold was constructed as shown in Scheme 2 by reacting ethyl-2-mercaptoacetate with 4,6-dichloro-5-formyl pyrimidine (**17**) to give compound **18**, which was reacted with aqueous ammonia at high temperature to afford key 2,4-diamino thienopyrimidine **16**.[76] Compound **18** underwent Suzuki cross coupling reactions[77] with commercially available boronic acids to furnish 4-aryl-2-aminopyrimidines **19a**−**e** (Scheme 3). Saponification of the ethyl esters **19a** and **19e** gave the corresponding acids **20a** and **20e**, which underwent a HATU mediated coupling with ethylamine hydrochloride to afford ethyl amides **21a** and **21e**. Alternatively, ethyl amides **21b**−**d** were made by direct conversion of the ethyl esters by heating with ethylamine in methanol solution. The 5′-aryloxy derivatives **34a**−**m** (Scheme 4) were made by a similar method, although the key intermediate **26** required the prior synthesis of an appropriate cross coupling partner. Thus, the commercially available nitro phenol **22** was protected with a benzyl group (**23**) and the nitro group then reduced to aniline **24**. Subsequent diazotization of the aniline followed by quenching the intermediate diazonium salt with iodine afforded iodophenol derivative **25**, which was then converted to an intermediate boronate ester via a palladium mediated process.[78] The

Table 3. Binding Affinity (FP Assay) and Antiproliferative Potency,[a,b] (GI_{50}) in Various Human Cancer Cell Lines for Compound **34a**

compd no.	human Hsp90β FP IC_{50} (μM)	HCT116 (colon) GI_{50} (μM)	BT474 (breast) GI_{50} (μM)	PC3 M (prostate) GI_{50} (μM)	A2058 (melanoma) GI_{50} (μM)	WM226.4 (melanoma) GI_{50} (μM)	A549 (lung) GI_{50} (μM)
34a	0.056	0.187	0.073	0.498	0.108	0.145	0.167

[a] Values are reported as the mean of at least two independent determinations. [b] Antiproliferative potency as indicated by concentrations which lead to 50% growth inhibition (GI_{50}) in a SRB assay.

Table 4. Measurement of Microsomal Turnover,[a] Plasma Protein Binding (PPB),[b] and Cytochrome P450 Inhibition[c] for Compound **34a**

	microsomal turnover (%)			PPB (% bound)			CYP450 IC_{50} (μM)				
compd no.	mouse	rat	human	mouse	rat	human	CYP 1A2	CYP 2C9	CYP 3A4	CYP 2D6	CYP 2C19
34a	19.3	16.9	17.3	90.7	90.1	96.2	> 10	> 10	> 10	> 10	0.34

[a] Data shown is the percent turnover of compound ($n = 3$) after a 10 min incubation of compound and NADPH. The results are expressed as percentage of controls without NADPH. [b] Measured by equilibrium dialysis after a 6 h incubation. [c] Values are reported as the mean of at least two independent determinations.

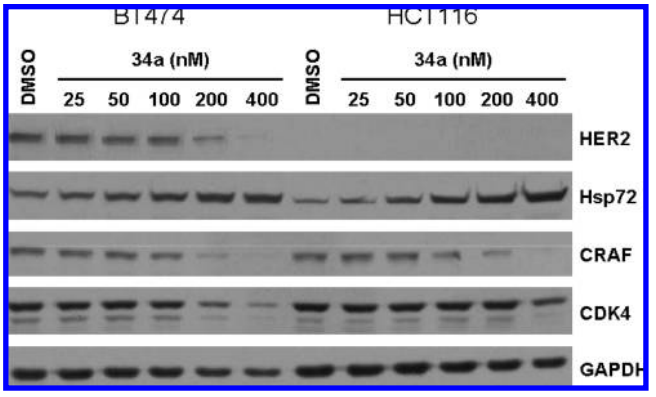

Figure 7. Effects of **34a** on expression of HER2, Hsp72, CRAF, and CDK4 in BT474 and HCT116 cells as determined by Western blot after 24 h. Compounds concentrations were 25, 50, 100, 200, and 400 nM concentrations. GAPDH was used as a loading control. Expression levels of HER2 in HCT116 cells are too low to be detected (consistent with etiology of this cell line).

boronate ester derivative of **25** underwent cross coupling with compound **18** (Scheme 2) to give compound **26**. It was found that only the ethyl amide **28** could be made by direct conversion from the ethyl ester **26**; other amides (**29** and **30**) were made via the carboxylic acid **27**. Boron trichloride mediated deprotection of benzyloxy compounds **28**−**30** gave corresponding phenols **31**−**33**, which were then derivatized to give **34a**−**i** by either reaction with alkyl halides or by Mitsunobu reactions[79] with the appropriate alcohols. An alternative approach to the construction of the thienopyrimidines **34** is shown in Scheme 5. In this case, compound **31** was reacted with 2-bromoethylacetaladehyde diethyl acetal to generate the acetal derivative **35**. In situ generation of the corresponding aldehyde and subsequent reductive amination reaction with appropriate amine and sodium triacetoxy borohydride afforded compounds **34j**−**m** (Scheme 5).

Results and Discussion

Compound **13** was considered a suitable start point for further medicinal chemistry optimization, and a series of close analogues was synthesized and evaluated as Hsp90 inhibitors (unpublished results). In addition, however, the structural information provided by **13** and that from **12** and the fragment screening hits (Figure 3) suggested the design of a novel chemotype. Overlays of the X-ray structures of fragment hits **10** and **11** with the in silico screening hits **12** and **13** led to the synthesis of compounds **14** and **15**. Compound **14** incorporated a phenyl substituent, similar to **12** and **13**, and compound **15** comprised an amide akin to **13**. From the X-ray structures of **12** and **13**, these groups were observed to make important contacts with the Hsp90 binding site (Figure 5). Thus, replacement of the methyl group in triazine **10** to a phenyl group in triazine **14** improved affinity in the FP assay from 350 to 20 μM. Similarly, modification of amino-pyrimidine hit **11** afforded **15** with a significant improvement in binding affinity from > 4000 to 535 μM (Table 1). Further examination of the X-ray structural information of fragment hits, close analogues, and the hits from the virtual screening campaign and associated structural information afforded by X-ray crystallography (Figure 5) led to the design of the 2-amino-thienopyrimidine scaffold exemplified initially by the 2,4-diaminothienopyrimidine **16** (Figure 6). Several salient features were apparent from the structural information.[80] In particular, the binding pose adopted by the fragment **10** was dependent on the experimental technique (soak versus cocrystallization) utilized for ligand−protein complex preparation (Figure 5). This highlights the subtleties of fragment−protein interactions and the value of obtaining multiple structures from diverse chemotypes. The binding mode of the aminothienopyrimidine core of compound **16** was consistent with that observed in crystals obtained via cocrystallization and was maintained in all subsequent analogues synthesized during the optimization phase. Interestingly, the binding mode for **10** obtained via ligand soak was reminiscent of that observed with the resorcinol inhibitor **5** (Figure 5), with the 2-amino moiety of the triazole mimicking the key interactions made by the 2-hydroxyl group in **5**. A further feature taken into account was the flexibility of the L107 residue, which adopts several ligand dependent orientations in the displayed data.

Although the affinity of compound **16** measured by FP assay was low (FP IC_{50} = 1250 μM; Table 1), we were confident from both structural information and the SAR available that incorporation of an aryl group at the 4-position of the 2-aminothieno[2,3-*d*]pyrimidine scaffold would lead to enhanced potency. A number of 4-aryl-2-aminothienopyrimidines were synthesized (Scheme 3) and indeed displayed greatly enhanced affinity for the protein target (Table 2). In addition, these compounds also inhibited the proliferation of cancer cell lines in vitro, as demonstrated by their GI_{50} values against a human colon carcinoma (HCT116) cell line (Table 2). The SAR (though limited) suggested that small lipophilic groups at the aryl 2′- and 4′-positions were advantageous in terms of affinity and antiproliferative effects. It seemed probable that further improvements in cell potency

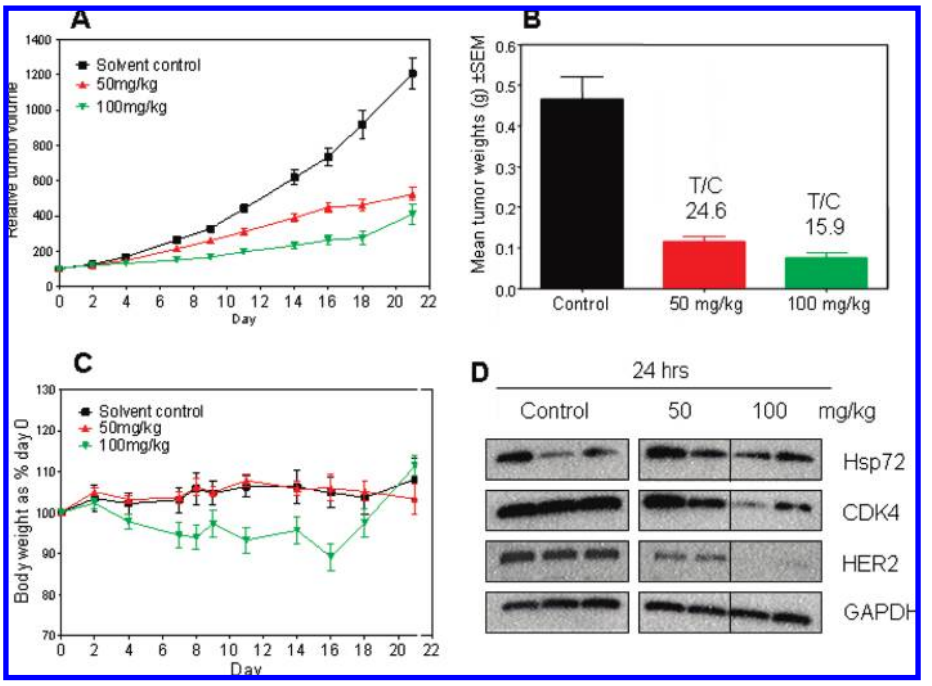

Figure 8. Response of established WM266.4 human melanoma xenografts to **34a** therapy (50 and 100 mg/kg, qd, po). (A) Relative tumor volumes (compared with volumes at start of therapy). Key: black squares, vehicle controls; red triangles, **34a** at 50 mg/kg po; green inverted triangles, **34a** at 100 mg/kg po. (B) Mean weights of excised tumors after 21 days therapy. (C) Mean mouse body weights during therapy. (D) Pharmacodynamic biomarker changes assessed by Western blotting (24 h after final dose).

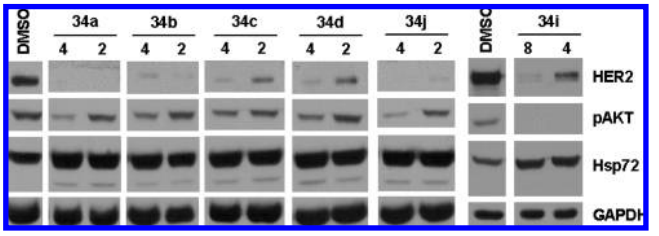

Figure 9. Effects of thienopyrimidines **34a**−**d** and **34i**−**j** on expression of HER2, pAKT, and Hsp72 in BT474 cells as determined by Western blot at 24 h. Cells were exposed to compounds **34a**−**d** and **34j** at 4 and 2 times GI_{50}, and compound **34i** was used at 8 and 4 times GI_{50}. GAPDH was used as a loading control.

could be effected by incorporation of a solubilizing group into the amino thieno[2,3-*d*]pyrimidine scaffold. The structural information gained from the X-ray crystal structure of compound **21e** (Figure 5; PDB code: 2WI6) suggested that the 5′-position of the thienopyrimidine 4-aryl substituent was a suitable position for such a solubilizing moiety. A powerful tenet of structure-based design is that it allows structural information from one chemotype to be applied to other distinct chemical series. Comparing the X-ray crystal structures of **21e** and the resorcinol inhibitor **5** (Figure 5; PDB code: 2VCI) provided support for the planned solubilizing group position, as the vector from the 5′-position would orient solubilizing groups to a similar spatial region (toward solvent) as that occupied by the morpholine solubilizing moiety in **5**. By using the 5′-phenolic hydroxyl group as a handle for chemical derivatization, the diethylaminoethyl compound **34a** was prepared (Scheme 4). Compound **34a** demonstrated enhanced affinity (FP $IC_{50} = 0.056\ \mu M$) for the protein target (that could be rationalized by structural data, vide infra) and, in addition, displayed greatly enhanced antiproliferative activity (as compared to **21e**), with a GI_{50} (HCT116) of $0.187\ \mu M$.

Furthermore, **34a** demonstrated potency against a wider range of cell lines as shown in Table 3. Evaluation of in vitro drug metabolism and pharmacokinetic (DMPK) parameters, including plasma protein binding (PPB), microsomal turnover (TO), and cytochrome P450 inhibition established an acceptable druglike profile for **34a** (Table 4). It was important to establish that the new compounds still retained the well-established molecular signature of known Hsp90 inhibitors on cellular biomarkers that would be indicative of target modulation (i.e., degradation of Hsp90 client proteins and up-regulation of the cochaperone Hsp72).[7] Figure 7 shows that the compound **34a** gave the expected depletion of the client proteins CRAF and CDK4 and induction of Hsp72 in BT474 and HCT116 cells in vitro in a concentration-dependent manner, as determined by Western immunoblotting. Depletion of the client protein HER2 (ErbB2) was observed for BT474 cells treated with **34a** though the expression levels of HER2 in HCT116 cells are too low to be predictive in this cell line, and thus no expression was seen even with control. These biomarker study results supported the premise that the effects on cell growth were a consequence of chaperone inhibition.

These data and the subsequent evaluation of compound plasma concentrations (Table 5) and compound tolerability following oral administration led to the selection of **34a** for a study of in vivo efficacy in a human cancer xenograft model. Thus **34a** was dosed at 50 and 100 mg/kg po daily to female Ncr athymic mice bearing established bilateral subcutaneous WM266.4 human melanoma tumors, a model we had previously shown to be responsive to NVP-AUY922.[52] Both dosing regimes demonstrated significant efficacy after 21 days of dosing. The values for percent treated/control ratio (*T*/*C*) were 24.6 and 15.9%, at doses of 50 and 100 mg/kg, respectively (Figure 8), indicating 75.4 and 84.1% inhibition of tumor growth. Evidence of tumor biomarker modulation was also observed in this study

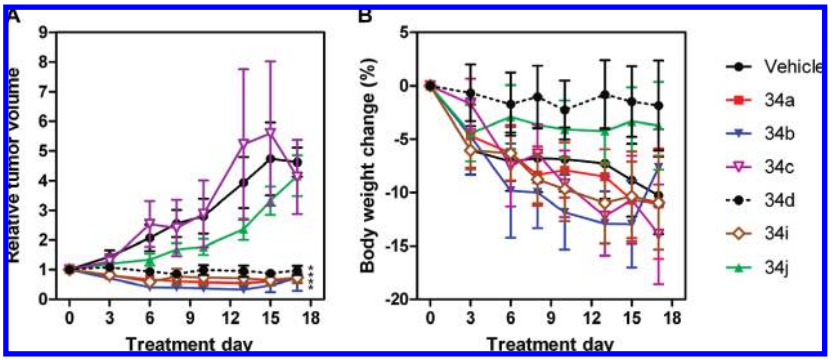

Figure 10. Response of established BT474 human breast cancer xenografts to therapy with thienopyrimidines **34a**−**d** and **34i**−**j** (30 mg/kg, qd, po). (A) Mean relative tumor volumes. (B) Mean body weight changes in % during therapy. Bars represent SEM * $p < 0.05$, one-way ANOVA post hoc Dunnet's.

Table 5. Binding Affinities[a] for Hsp90, Antiproliferation Potency[b], and Pharmacokinetic Parameters[c] for Selected 2-Aminothieno[2,3-*d*]pyrimidines

compd no.	FP IC_{50} (μM)	GI_{50} (BT474) (μM)	AUC_{last} (ng·h/mL)	C_{max} (ng/mL)	T_{max} (h)	half life (h)
34a	0.056	0.073	858	238	0.5	2.2
34b	0.064	0.075	622	160	2.0	2.6
34c	0.047	0.095	4831	702	1.0	5.3
34d	0.058	0.053	1155	380	2.0	2.5
34e	0.127	0.072	125	437	0.25	0.1
34f	0.08	0.072	1354	396	2	1.6
34g	0.029	0.135	*d*	*d*	*d*	*d*
34h	0.080	0.047	*e*	*e*	*e*	*e*
34i	0.176	0.089	1222	370	1	2.5
34j	0.087	0.097	1698	153	4.0	3.1
34k	0.102	0.088	854	304	2.0	1.7
34l	0.084	0.103	956	328	2.0	1.4
34m	0.058	0.134	208	170	0.25	0.8

[a] Measured by FP assay, mean of at least two determinations. [b] GI_{50} values in a human breast cancer cell line (BT474), mean of at least two determinations. [c] Plasma pharmacokinetics generated following a 10 mg/kg oral dose to male Balb-c mice. [d] Not reported. Compound was only detected in a few samples (0.5 to 2 h) all below the limit of quantification (LLoQ 50 ng/mL). [e] Not reported; compound only detected above the LLoQ, (50 ng/mL) at 15 min with a concentration of 296 ng/mL.

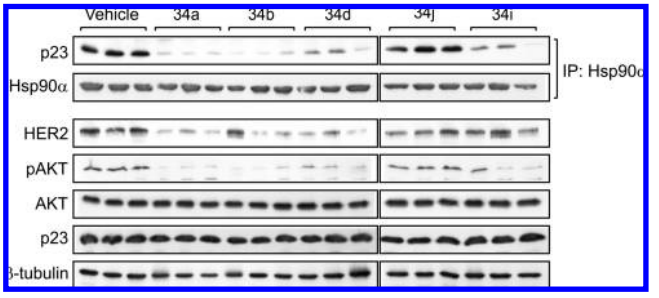

Figure 11. Tumor pharmacodynamic biomarker changes in nude mice bearing established BT474 human breast cancer xenografts following daily dosing of at 30 mg/kg of **34a**, **34b**, **34d**, **34j** or **34i**. BT474 tumors were collected from treated nude mice at the end of the efficacy experiment and assayed for either dissociation of p23 from Hsp90α or for client protein degradation (6 h after final dose).

(Figure 8). The 50 mg/kg dose was well tolerated, with no significant body weight loss over the treatment period; the 100 mg/kg dose was less well tolerated, however, resulting in body weight loss and several dosing interruptions. Compound **34a** also showed good activity in the PC3 human prostate cancer xenograft model in which the tumors were grown orthotopically in the mouse prostate gland. Daily (po) doses of 50 and 100 mg/kg of **34a** gave *T*/*C* values of 23.0 and 19.9%, respectively (77.0 and 80.1% inhibition), with similar inhibition of local and distal lymph node metastases and evidence of biomarker modulation (data in Supporting Information).

These promising early findings led to synthesis and evaluation of analogues of **34a**. On the basis of binding affinity, antiproliferative potency, and in vitro DMPK properties, a further 12 compounds (Scheme 4 and Scheme 5, **34b**−**m**) were selected for oral pharmacokinetic (PK) studies in mice with a view to selecting compounds with an appropriate profile for additional pharmacodynamic biomarker studies and tumor xenograft efficacy experiments. Table 5 shows binding affinity, antiproliferative data in a BT474 human breast cancer cell line (previously shown to be responsive to NVP-AUY922),[52] and pharmacokinetic data following oral dosing at 10 mg/kg for compounds **34a**−**m**. The ability of this set of analogues to modulate pharmacodynamic biomarkers in BT474 breast cancer cells was also determined. All 13 compounds listed in Table 5 induced Hsp72 and significantly reduced HER2 expression as well as decreasing the levels of the Hsp90 client protein pAKT (Ser473 phosphorylated AKT) at concentrations of between 2 and 8 times their GI_{50}. A subset of these results (for **34a**−**d** and **34i**−**j**) is shown in Figure 9. In these examples, pharmacodynamic biomarkers are affected at compound concentrations of 2 and/or 4 times GI_{50} for compounds **34a**−**d** and **34j** and at 4 and 8 times GI_{50} for compound **34i**. Analysis of these and other profiling data such as microsomal stability (human, rat and mouse), hepatic clearance, and potency against cytochrome P450 isoforms led to the selection of compounds **34a**−**d** and **34i**−**j** for evaluation in a human BT474 breast cancer xenograft model in vivo. The effects of these compounds on the growth of established

Table 6. Tumor and Host Responses of BT474 Human Breast Cancer Xenograft Bearing Nude Mice to **34a**−**d** and **34i**−**j** Therapy[a]

	tumor response			host response		
compd no.	T/C (%)	regression (%)	Δ tumor vol[b] (mm^3)	Δ body wt (g)	Δ body wt (%)	survival (alive/total)
vehicle	100		372 ± 52	−3.0 ± 1.0	−11 ± 3.6	8/8
34a		28.4	−29 ± 12	−3.1 ± 1.5	−11 ± 5.2	7/8
34b		15.6	−15 ± 47	−2.3 ± 1.1	−7.8 ± 3.6	4/8
34c	85		316 ± 121	−4.1 ± 1.3	−14 ± 4.7	6/8
34d		3.0	−3 ± 15	−0.7 ± 1.3	−2.3 ± 4.2	8/8
34i		27.4	−28 ± 13	−3.2 ± 1.3	−11 ± 4.4	8/8
34j	90		336 ± 66	−1.1 ± 1.1	−3.8 ± 4.1	8/8

[a] The animals were dosed orally once per day at 30 mg/kg in a dose volume of 10 mL/kg. Vehicle was 0.5% sodium carboxymethyl-cellulose. [b] Treatment was initiated when the average tumor volume reached approximately 100 mm^3.

Table 7. Binding Affinity (FP Assay) and Antiproliferative Potency (GI_{50}) in Various Human Cancer Cell Lines for Compound **34d**[a]

compd no.	human Hsp90β FP IC_{50} (μM)	HCT116 (colon) GI_{50} (μM)	MCF7 (breast) GI_{50} (μM)	PC3 M (prostate) GI_{50} (μM)	A375 (melanoma) GI_{50} (μM)	T24 (bladder) GI_{50} (μM)	U87MG (glioma) GI_{50} (μM)
34d	0.058	0.120	0.118	1.05	0.038	0.145	0.857

[a] Values are reported as the mean of at least two independent determinations.

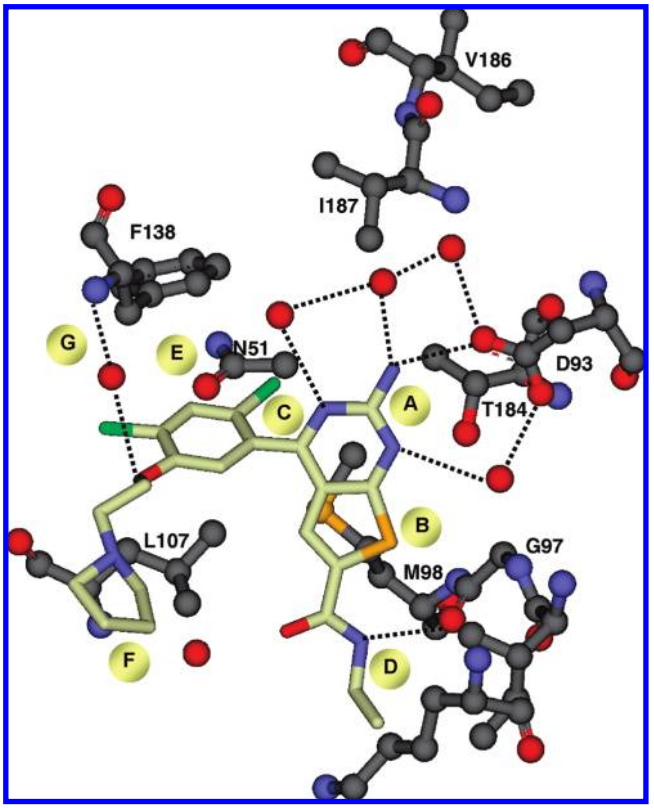

Figure 12. Detail of the X-ray structure of compound **34d** bound to the ATP binding site of the N-terminal domain of human Hsp90α (PDB code: 2WI7), showing selected amino acids and listing key ligand−protein interactions (note main chain atoms of N51 removed for clarity). Red spheres represent structurally conserved water molecules with key hydrogen bonding network shown as dotted lines. (A) Key H-bonds (to water and D93); (B) thieno-ring stacking with M98; (C) chlorine filling small amphiphilic pocket; (D) H-bond interaction with G97; (E) lipophilic interaction with L107/F138 and stacking with N51; (F) solvent exposed; (G) water-mediated H-bond to F138.

BT474 human breast cancer xenografts are shown in Figure 10 and Table 6. Four of the compounds were efficacious in this model following once daily oral dosing at 30 mg/kg, and indeed, **34a**, **34b**, **34d** and **34i** caused tumor regressions of up to 28% (Table 6). Two compounds (**34c** and **34j**) were not efficacious in this model, and two compounds (**34c** and **34b**) were not well tolerated using the selected dosing regime (Table 6). For all four of the compounds that caused tumor regression, the expected mechanism-based pharmacodynamic biomarker responses were seen in the tumor tissues, indicative of Hsp90 inhibition (Figure 11). These included the abrogation of the interaction between Hsp90 and p23, the degradation of HER2, and a decrease in levels of pAKT. In contrast, **34j**, which did not inhibit tumor cell growth in BT474 xenograft model, appeared to effect less robust pharmacodynamic biomarker changes (Figure 11) despite high plasma exposure (Table 5). As **34j** affected pharmacodynamic markers in vitro and displayed equivalent in vitro potency, it could be surmised that the compound did not attain appropriate tumor exposure, although in the absence of measured tumor concentrations for this particular study, this hypothesis was not confirmed. Overall, the tumor pharmacodynamic data shown in Figure 11 (and that from corresponding in vitro studies) support the notion that the tumor regression observed with four thienopyrimidines, **34a**, **34b**, **34d** and **34i** is due to inhibition of Hsp90 ATPase enzymatic activity.

Compound **34d** displayed potent antiproliferative effects in a wide range of cell lines covering different human cancer subtypes and genetic abnormalities; the GI_{50} values for a representative selection are shown in Table 7. The binding mode of compound **34d** was established by X-ray crystallography and, as expected, this was consistent with that seen previously for the 2-amino thieno[2,3-*d*] pyrimidine compound **21c** (Figure 5). The potency of **34d** and related analogues can be rationalized by the key interactions the compounds make with the protein within the N-terminal ATP binding site (Figure 12). Compound **34d** makes several water-mediated hydrogen bonding interactions with D93. This critical interaction is seen in the structure of Hsp90 complexed with ADP[18] and indeed all reported Hsp90 inhibitors where structural information is available.[5] The amide functionality also makes a direct hydrogen bond interaction with G97, mirroring that seen with the amide moiety of compound **5** and Hsp90. Key hydrophobic interactions include those with L107, F138 and stacking with N51. The 2′-chloro substituent on the aryl ring induces the two rings to adopt an appropriate angular relationship, which allowed the 2′-chloro to bind in a small lipophilic pocket, displacing a water molecule normally resident. This feature may provide a

rationale for the increased binding affinity seen for **21c**, **21d**, and **21e** over **21a**. Another important water-mediated-interaction is that between the 5′ phenolic oxygen and carbonyl of F138 (interaction G in Figure 12). This interaction can be inferred to explain the improved potency of 5′-aryl-alkoxy compounds such **34a** (FP $IC_{50} = 0.056\ \mu M$) over compounds such as **21e** (FP $IC_{50} = 0.230\ \mu M$), which cannot make this interaction. These affinity data and the structural information pertaining to **21c**, **34d** and related compounds clearly demonstrate the importance of conserved structural water molecules to ligand-protein interaction for Hsp90 inhibitors.

Conclusion

Several weakly binding Hsp90 inhibitors from distinct chemical classes were identified by a combination of fragment and in silico screening technologies. Analysis of the X-ray structures of these compounds and other inhibitors bound to Hsp90 allowed the design of a novel and orally active 2-aminothieno[2,3-*d*]pyrimidine class of Hsp90 inhibitor. Compounds from this series displayed binding affinity in the 50−100 nM range, as measured by a FP binding assay and significantly inhibited cell proliferation in a wide range of human cancer cell lines. The characteristic molecular biomarker signature of Hsp90 inhibition was seen in vitro and in vivo for active members of this series, and good exposure levels were obtained following oral administration. Statistically significant efficacy was observed in a subcutaneous BT474 human breast tumor xenograft model for compounds **34a**, **34b**, **34d** and **34i** when dosed orally qd at 30 mg/kg. This work demonstrates the rapid identification of novel orally active Hsp90 inhibitors from a structure-based research program, which combined elements from various hit identification approaches. Compound **34d** (NVP-BEP800/VER-82576[81]) has been selected for further development and additional characterization of **34d**, and compounds from this series will be reported elsewhere.

Experimental Section

Fluorescence Polarization Assay. The ability of compounds to compete with a fluorescently labeled probe for binding to full length human Hsp90β was determined as described previously[74] with a modified probe (VER-00051001). This probe binds with greater affinity to Hsp90 than that described previously, allowing the accurate determination of IC_{50} for higher affinity compounds. Synthetic procedures for VER-00051001 and details relating to the FP assay can be found in the Supporting Information.

Cell Growth and Client Protein Degradation. Growth inhibition assays using the SRB method were undertaken as previously described.[29] Client protein degradation was determined by Western blotting. In brief, HCT116 cells were exposed to compounds **34a**−**d** and **34i**−**j** at 2, 4, or 8 times their cellular GI_{50} for 24 h. Cell lysates were prepared in 50 mM Tris-HCl, 2% SDS pH6.8, and protein levels determined by the BCA method (Pierce, Rockford, IL). Equal amounts of lysate were separated by SDS-PAGE and proteins transferred to PVDF membrane. Her2 (ab8054, Abcam), Raf-1 (sc-133, Santa Cruz Biotechnology), and Hsp72 (SPA-810, StressGen) were determined using ECL (GE Bioscience). GAPDH (MAB374, Chemicon International) levels were determined to show equal protein loading.

Pharmacokinetics. Male Balb-c mice received a single 10 mg/kg dose of compound via oral gavage in 1% methyl cellulose (w/v). Plasma was prepared from terminal blood samples for analysis. LC-MS/MS was used for quantitative bioanalysis, and pharmacokinetic analysis was performed using WinNonLin (Pharsight).

Plasma Protein Binding Measurements. Plasma protein binding was determined by equilibrium dialysis using a HTDialysis 96-well Teflon block. Compounds were incubated in plasma at 5 μM for 6 h. Plasma and buffer samples were protein precipitated with acetonitrile and the supernatants analyzed by LC/MSMS. Percent bound was calculated as $(1 - (\text{buffer}/\text{plasma})) \times 100$.

Microsomal Stability Studies. Compounds were incubated in liver microsomes (0.5 mg/mL) at 1 μM for 10 min ± 2 mM NADPH. Samples were protein precipitated with acetonitrile and centrifuged, and supernatants were analyzed by LC/MSMS. Turnover was calculated as percent of control samples without NADPH. The experiment was carried out with liver microsomes from three different species (a human mixed pool, C57 mouse and SD rat).

Efficacy Study in WM266.4 Melanoma Xenografts. All work was performed in accordance with the Home Office regulations under the Animals (Scientific Procedures) Act 1986 and UKCCCR guidelines.[82] Female Ncr athymic mice 6−8 weeks of age bred in-house were inoculated bilaterally sc with 2 million BRAF mutant human WM266.4 melanoma cells. Therapy with **34a** commenced on day 6 following tumor cell implantation when tumors were approximately 5 mm mean diameter. Mice were randomized into three groups of 9−10 animals. The compound was dissolved in DMSO and diluted in sterile saline/Tween 20 such that animals received the dose required in 0.1 mL of final solution per 10 g body weight. Final concentrations were DMSO, 10%; Tween 20, 5%; saline: 85%. Controls received an equal volume of vehicle. Animals were dosed daily at 50 or 100 mg/kg compound by oral gavage. Dosing continued until day 21 except for some variations in schedule to allow for body weight loss recovery. Mice receiving 100 mg/kg group were not dosed on days 6, 8, 11, and 16−19. Two mice were culled from the latter group on day 8 and 16 due to loss of condition. Tumor measurements and body weights were recorded three times weekly. The study was terminated on day 21. Cohorts of animals were culled 6, 16, and 24 h after the final dose of compound. Tumors were excised and weighed, and plasma and tumor samples frozen for pharmacokinetic and pharmacodynamic analyses (by Western blotting) as previously described.[52]

Efficacy Study in BT474 Human Breast Cancer Xenografts. The ER positive, HER2 overexpressing human breast ductal carcinoma cell line BT-474 was purchased from American Type Culture Collection (HTB-20, Manassas, VA). The cells were grown in DMEM high glucose (4.5 g/L) supplemented with 10% FCS, 200 mM L-glutamine, and 1% sodium pyruvate (BioConcept, Allschwil, Switzerland). Two or three days prior to cell inoculation, each mouse was subcutaneously implanted on the upper dorsal side with a 17β-estradiol pellet (25 μg/day, 90 day release, Innovative Research of America, FL) using a trocar needle. BT-474 cells (5×10^6) were injected in 200 μL Matrigel:HBSS (1:1 vol) (BD Matrigel Basement Membrane Matrix, BD Biosciences, CA) subcutaneously in the right flank. Treatment was initiated when the average tumor volume reached approximately 100 mm^3. Tumor growth and body weights were monitored at regular intervals. The xenograft tumor sizes were measured manually with calipers, and the tumor volume was estimated using the formula: $(W \times L \times H \times \pi/6)$, where width ($W$), height ($H$), and length ($L$) are the three largest diameters. Invasive procedures were performed under Forene anesthesia. All experiments were performed using female Harlan HsdNpa: athymic Nude-nu mice which were obtained from Novartis internal breeding stocks (Laboratory Animal Services, Novartis Pharma AG, Basel, Switzerland). The animals were kept under optimized hygienic conditions (OHC) with a 12 h dark, 12 h light conditions. The animals were fed food and water ad libitum. All animal experiments were performed in strict adherence to the Swiss law for animal

protection. The experimental protocols were approved by the Swiss Kantonal Veterinary Office of Basel Stadt.

Chemistry. Tested compounds are >95% chemical purity as measured by HPLC (except where stated in the experimental characterization for a particular compound). All compounds tested in vivo are >95% purity. The methods for HPLC analysis and a table of data for all tested compounds is provided in the Supporting Information.

4-Methylsulfanyl-6-phenyl-[1,3,5]-triazin-2-ylamine (14). Dimethyl cyanodithioiminocarbonate (Acros, 100 mg, 0.68 mmol) and benzamidine hydrochloride (107 mg, 0.68 mmol) were suspended in EtOH (3 mL), and diisopropylethylamine (0.24 mL, 1.38 mmol) was added. The reaction mixture was heated to 65 °C for 3.5 h. The mixture was allowed to cool to ambient temperature, and the solvents were then removed in vacuo. The residual product was purified by flash chromatography on silica gel, eluting with DCM to afford the title compound **14** (45 mg, 30%) as a colorless solid: TLC $R_f = 0.59$ (MeOH/DCM 1:19); LCMS $t_R = 2.10$ min; $m/z = 219$ $[M + H]^+$. ^{1}H NMR (400 MHz, DMSO-d_6) δ 2.52 (s, 3H), 7.48−7.54 (m, 2H), 7.55−7.63 (m, 3H), 8.29−8.32 (m, 2H). ^{13}C NMR (100.6 MHz, DMSO-d_6) δ 12.6 (CH_3), 128.0 (CH), 128.5 (CH), 132.1 (CH), 135.6 (C), 165.6 (C), 168.7 (C), 180.7 (C). HRMS, calcd for $C_{10}H_{10}N_4S$ $[M + H]^+$ 219.0704, found 219.0707. HPLC (method C) 99.4% ($t_R = 1.18$ min).

2-(2-Amino-6-methyl-pyrimidin-4-ylsulfanyl)-*N*-methylacetamide (15). A mixture of 2-amino-4-chloro-6-methylpyrimidine (144 mg, 1.0 mmol), 2-mercapto-*N*-methyl acetamide (105 μL, 1.2 mmol), and triethylamine (167 μL, 1.2 mmol) in MeOH (3 mL) was heated in a microwave synthesizer at 120 °C for 10 min. The reaction mixture was cooled to ambient temperature, and the solvents were then removed in vacuo. The solid residue was purified by preparative HPLC (at pH 4) to afford the title compound **15** (20 mg, 9%) as a colorless solid: LCMS $t_R = 0.45$ min; $m/z = 213$, $[M + H]^+$. ^{1}H NMR (400 MHz; DMSO-d_6) δ 2.13 (s, 3H), 2.59 (d, 3H, $J = 4.5$ Hz), 3.73 (s, 2H), 6.40 (s, 1H), 6.60 (brs, 2H), 7.96 (brq, 1H). ^{13}C NMR (100.6 MHz, DMSO-d_6) δ 23.3 (CH_3), 26.0 (CH_3), 31.9 (CH_2), 105.6 (CH), 162.4 (C), 166.0 (C), 167.9 (C), 168.0 (C). HRMS, calcd for $C_8H_{12}N_4OS$ $[M + H]^+$ 213.0810, found 213.0804. HPLC (method C) 99.3% ($t_R = 0.55$ min).

2-Amino-4-chloro-thieno[2,3-*d*]pyrimidine-6-carboxylic Acid Ethyl Ester (18). Ethyl-2-mercaptoacetate (2.86 mL, 26 mmol) was added dropwise to a suspension of 2-amino-4,6-dichloro-5-pyrimidine carbaldehyde (**17**) (Bionet Research Intermediates, UK; 5.0 g, 26 mmol) and K_2CO_3 (9.0 g, 65.2 mmol) in MeCN (160 mL). The mixture was heated to 85 °C for 5 h and then allowed to cool to ambient temperature. The mixture was filtered, and the filtered solids were washed with MeCN (2 × 50 mL) and then water (2×50 mL) and dried in vacuo at 60 °C to afford the title compound **18** (5.52 g, 82%) as a yellow solid: LCMS $t_R = 2.37$ min; $m/z = 260$, 258 $[M + H]^+$. ^{1}H NMR (400 MHz; DMSO-d_6) δ 2.09 (t, 3H, $J = 7.0$ Hz), 4.31 (q, 2H, $J = 7.0$ Hz), 7.70 (brs, 2H), 7.78 (s, 1H).

2,4-Diaminothieno[2,3-*d*]pyrimidine-6-carboxylic Acid Amide (16). 2-Amino-4-chloro-thieno[2,3-*d*]pyrimidine-6-carboxylic acid ethyl ester (**18**) (257 mg, 1.0 mmol) was suspended in aq ammonia solution (5 mL) then heated at 130 °C in a microwave synthesizer for 15 min. The reaction mixture was allowed to cool and concentrated in vacuo. The residue was purified by preparative HPLC (at pH 4) to afford the title compound **16** (45 mg, 22%) as a colorless solid: LCMS $t_R = 0.74$ min; $m/z = 210$, $[M + H]^+$. ^{1}H NMR (400 MHz; DMSO-d_6) δ 6.29 (brs, 2H), 7.08 (brs, 2H), 7.2−7.4 (brs, 1H), 7.5−7.8 (brs, 1H), 7.82 (s, 1H). HRMS, calcd for $C_7H_7N_5O_5$ $[M + H]^+$ 210.0450, found 210.0457. ^{13}C NMR (100.6 MHz; DMSO-d_6) δ 109.0 (C), 123.0 (CH), 125.9 (C), 159.8 (C), 161.8 (C), 163.7 (C), 170.6 (C). HPLC (method C) 100% ($t_R = 0.29$ min).

2-Amino-4-phenylthieno[2,3-*d*]pyrimidine-6-carboxylic Acid Ethyl Ester (19a). Phenylboronic acid (2.25 g, 18.5 mmol) was added to a mixture of 2-amino-4-chloro-thieno[2,3-*d*]pyrimidine-6-carboxylic acid ethyl ester **18** (3.65 g, 14.2 mmol) and $NaHCO_3$ (3.56 g, 42.6 mmol) in DMF (66 mL) and water (11 mL). The mixture was degassed by evacuation−nitrogen purge (three cycles), followed by bubbling nitrogen gas through the reaction mixture for 10 min. Dichlorobis(triphenylphosphine)palladium(II) catalyst (650 mg, 5 mol %) was added, and the reaction mixture was heated under a nitrogen atmosphere at 80 °C for 5.5 h. The mixture was cooled, solvents were removed in vacuo, and the residue partitioned between water (100 mL) and EtOAc (100 mL). This mixture was filtered through a pad of celite 521, and the filtrate phases were separated. The organic phase was washed with water (100 mL) and then sat. aq NaCl solution (100 mL) and dried over anhydrous Na_2SO_4 and filtered. The filtrate solvents were removed in vacuo, and the crude product was purified by flash chromatography on silica gel (50 g) eluting with a gradient of 10−50% EtOAc/hexane to afford the title compound **19a** (2.67 g, 63%) as a yellow solid: LCMS $t_R = 2.57$ min; $m/z = 300$ $[M + H]^+$. ^{1}H NMR (400 MHz; DMSO-d_6) δ 1.29 (t, 3H, $J = 7.1$ Hz), 4.30 (q, 2H, $J = 7.1$ Hz), 7.39 (brs, 2H), 7.58−7.62 (m, 3H), 7.83−7.89 (m, 2H) 7.87 (s, 1H).

2-Amino-4-phenylthieno[2,3-*d*]pyrimidine-6-carboxylic Acid (20a). Sodium hydroxide (134 mg, 3.35 mmol) was added to a suspension of 2-amino-4-phenyl-thieno[2,3-*d*]pyrimidine-6-carboxylic acid ethyl ester (**19a**; 200 mg, 0.67 mmol) in EtOH (10 mL) and water (2 mL). The mixture was heated to reflux for 45 min (affording a homogeneous solution) and then allowed to cool. EtOH was removed in vacuo and further water (20 mL) added. The residue pH was adjusted to 1 by dropwise addition of conc HCl. The resulting precipitate was filtered and then washed sequentially with water, EtOH, and diethyl ether and dried in vacuo to afford the title compound **20a** (130 mg, 72%) as a gray solid: LCMS $t_R = 1.79$ min; $m/z = 272$ $[M + H]^+$. ^{1}H NMR (400 MHz, DMSO-d_6) δ 7.32 (brs, 2H), 7.56−7.62 (m, 3H), 7.83 (s, 1H), 7.84−7.88 (m, 2H), 13.41 (brs, 1H).

2-Amino-4-phenylthieno[2,3-*d*]pyrimidine-6-carboxylic Acid Ethylamide (21a). 2-Amino-4-phenyl-thieno[2,3-d]pyrimidine-6-carboxylic acid (50 mg, 0.18 mmol) was dissolved in DMF (3 mL) and *O*-(7-azabenzotriazolo-1-yl)-*N*,*N*,*N*′,*N*′-tetramethyluroniumhexafluorophosphate (HATU; 77 mg, 0.2 mmol) was added followed by ethylamine hydrochloride (23 mg, 0.27 mmol) and diisopropylethylamine (96 μL, 0.54 mmol). The reaction mixture was heated to 100 °C for 10 min in a microwave synthesizer. The mixture was cooled, poured into water, and extracted with EtOAc (25 mL). The phases were separated, and the organic phase was washed with water (2 × 20 mL) then sat. aq NaCl (2×20 mL) and dried over Na_2SO_4. The mix was filtered, the filtrate solvent removed in vacuo, and the resulting residue purified by flash chromatography on silica gel (5 g) eluting with a gradient of 20−100% EtOAc/hexane to afford the title compound **21a** (31 mg, 59%) as a yellow solid: LCMS $t_R = 2.07$ min; $m/z = 299$ $[M + H]^+$. ^{1}H NMR (400 MHz; DMSO-d_6) δ 1.11 (t, 3H, $J = 7.2$ Hz), 3.26 (m, 2H), 7.14 (brs, 2H), 7.57−7.63 (m, 3H), 7.84−7.89 (m, 2H), 8.03 (s, 1H), 8.71 (t, 1H, $J = 5.5$ Hz). ^{13}C NMR (100.6 MHz, DMSO-d_6) δ 14.8 (CH_3), 34.0 (CH_2), 119.8 (C), 121.8 (CH), 128.7 (CH), 128.8 (CH), 130.3 (CH), 132.1 (C), 137.2 (C), 161.1 (C), 161.2 (C), 163.2 (C), 172.0 (C). HRMS calcd for $C_{15}H_{14}N_4OS$ $[M + H]^+$ 299.0967, found 299.0969. HPLC (method C) 100% ($t_R = 1.05$ min).

2-Amino-4-(2,4-dimethylphenyl)thieno[2,3-*d*]pyrimidine-6-carboxylic Acid Ethyl Ester (19c). This compound was made using the synthetic procedure described for compound **19a**. Thus 2,4-dimethylphenylboronic acid (1.06 g, 7.06 mmol) was reacted with 2-amino-4-chloro-thieno[2,3-*d*]pyrimidine-6-carboxylic acid ethyl ester **18** (1.401 g, 5.43 mmol). The crude product was purified by flash chromatography on silica gel (50 g) eluting with a gradient of 10−50% EtOAc/hexane to afford the title compound **19c** (1.11 g, 63%) as an off-white solid: TLC $R_f = 0.48$ (1:1 EtOAc/hexane). LCMS $t_R = 2.73$ min;

$m/z = 328$ $[M + H]^+$. ^{1}H NMR (400 MHz, DMSO-d_6) δ 1.26 (t, 3H, $J = 7.1$ Hz), 2.21 (s, 3H), 2.36 (s, 3H), 4.15 (q, 2H, $J = 7.1$ Hz), 7.16 (d, 1H, $J = 7.8$ Hz), 7.20 (s, 1H), 7.27 (d, 1H, $J = 7.8$ Hz), 7.36 (brs, 2H), 7.37 (s, 1H).

2-Amino-4-(2,4-dimethylphenyl)thieno[2,3-*d*]pyrimidine-6-carboxylic Acid Ethylamide (21c). 2-Amino-4-(2,4-dimethylphenyl)-thieno[2,3-*d*]pyrimidine-6-carboxylic acid ethyl ester **19c** (353 mg, 1.07 mmol) was suspended in ethylamine in methanol solution (2.0 M, 4 mL, 8.0 mmol) and the mixture was heated in a sealed vial (Caution) at 85 °C for 18 h. The reaction mixture was cooled to 0 °C, the vial was opened, and the solvents were removed in vacuo. The solid residue was purified by flash chromatography on silica gel (10 g) eluting with a gradient of 25−70% EtOAc/hexane to afford the title compound **21c** (252 mg, 72%) as a colorless solid: TLC $R_f = 0.19$ (1:1 EtOAc/hexane); LCMS $t_R = 2.28$ min; $m/z = 327$ $[M + H]^+$. ^{1}H NMR (400 MHz; DMSO-d_6) δ 1.06 (t, 3H, $J = 7.1$ Hz), 2.20 (s, 3H), 2.36 (s, 3H), 3.21 (m, 2H), 7.10 (brs, 2H), 7.16 (d, 1H, $J = 7.9$ Hz), 7.20 (s, 1H), 7.26 (d, 1H, $J = 7.9$ Hz), 7.56 (s, 1H)7.36 (brs, 2H), 7.37 (s, 1H), 8.60 (brt, 1H, $J = 5.6$ Hz). ^{13}C NMR (100.6 MHz; DMSO-d_6) δ 14.7 (CH_3), 19.5 (CH_3), 20.8 (CH_3), 34.0 (CH_2), 121.4 (C), 121.7 (CH), 126.4 (CH), 129.0 (CH), 131.2 (CH), 132.0 (C), 134.0 (C), 135.2 (C), 138.5 (C), 161.0 (C), 161.1 (C), 165.1 (C), 171.2 (C). HRMS calcd for $C_{17}H_{18}N_4OS$ $[M + H]^+$ 327.1280, found 327.1284. HPLC (method A) 98.6% ($t_R = 4.10$ min).

1-Benzyloxy-2,4-dichloro-5-nitrobenzene (23). Potassium carbonate (12 g, 87 mmol) was added to a solution of 2,4-dichloro-5-nitrophenol (**22**, Lancaster Synthesis, Morecambe, Lancashire, UK; 15.6 g, 75 mmol) in acetone (200 mL). Benzyl bromide (9.0 mL, 76 mmol) was added and the suspension heated at reflux for 18 h. The resulting suspension was allowed to cool, water (500 mL) was added, and the mixture was extracted with DCM (2×200 mL). The combined extracts were washed sequentially with aq sodium hydroxide (2.0 M; 150 mL), water (2×200 mL) and sat. aq NaCl solution (150 mL). The solution was dried over anhydrous Na_2SO_4 and concentrated in vacuo to afford the title compound **23** (21.5 g, 96%) as a pale-yellow solid: TLC $R_f = 0.73$ (DCM); LCMS $t_R = 2.92$ min; $m/z =$ no ionization. ^{1}H NMR (400 MHz; $CDCl_3$) δ 5.20 (s, 2H), 7.34−7.51 (m, 5H), 7.56 (s, 1H), 7.58 (s, 1H).

5-Benzyloxy-2,4-dichlorophenylamine (24). Iron powder (21 g, 376 mmol) was added to a suspension of 1-benzyloxy-2,4-dichloro-5-nitrobenzene (**23**; 21.5 g, 72 mmol) in acetic acid (300 mL) and water (150 mL) and the mixture was heated at 85 °C (oil bath temperature) for 90 min. The resulting suspension was filtered while still hot and then allowed to cool. Water (750 mL) was added and the mixture extracted with DCM (3× 150 mL). The combined extracts were washed with aq sodium hydroxide (2.0 M, 300 mL), water (2×500 mL), and sat. aq NaCl solution (200 mL). The solution was dried over anhydrous Na_2SO_4, filtered, and the filtrate solvents removed in vacuo to afford the title compound **24** (18.6 g, 96%) as a pale-brown solid: TLC $R_f = 0.57$ (DCM); LCMS $t_R = 2.79$ min; $m/z = 270$, 268 $[M + H]^+$. ^{1}H NMR (400 MHz, $CDCl_3$) δ 5.20 (s, 2H), 7.34−7.48 (m, 5H), 7.56 (s, 1H), 7.58 (s, 1H).

1-Benzyloxy-2,4-dichloro-5-iodobenzene (25). Hydrochloric acid (6.0 M, 60 mL) was added to a solution of 5-benzyloxy-2,4-dichlorophenylamine (**24**; 16.2 g, 60 mmol) in acetic acid (240 mL) and the resulting suspension cooled (ice/water/salt bath). A solution of sodium nitrite (4.8 g, 69.5 mmol) in water (40 mL) was added slowly (keeping the internal temperature < 5 °C). On complete addition, the resulting solution was stirred for 30 min and then the resulting solution was poured into a solution of potassium iodide (20 g, 120 mmol) and iodine (4 g, 16 mmol) in water (200 mL), and the mixture was stirred for 90 min. Water (800 mL) was added and the mixture extracted with dichloromethane (3 × 250 mL). The combined extracts were washed with 10% (w/v) aq sodium thiosulfate solution (2×150 mL), aq sodium hydroxide (2.0 M; 250 mL), water (2×250 mL), and sat. aq sodium chloride solution (200 mL). The solution was dried over anhydrous Na_2SO_4 and concentrated in vacuo to afford the title compound **25** (20.6 g, 90%) as a pale-brown solid: TLC: $R_f = 0.82$ (DCM); LCMS $t_R = 3.08$ min; $m/z =$ no ionization. ^{1}H NMR (400 MHz; $CDCl_3$) δ 5.10 (s, 2H), 7.33−7.48 (m, 7H).

2-Amino-4-(5-benzyloxy-2,4-dichlorophenyl)thieno[2,3-*d*]pyrimidine-6-carboxylic Acid Ethyl Ester (26). Potassium acetate (16 g, 163 mmol) was added to a solution of 1-benzyloxy-2,4-dichloro-5-iodo-benzene (**25**, 20.6 g, 54 mmol) and bis-(pinacolato)diboron (Boron Molecular; 14.5 g, 57 mmol) in DMF (50 mL) under a nitrogen atmosphere. Palladium acetate (450 mg, cat.) was added and the mixture heated at 90 °C (oil bath temperature) for 18 h. The resulting solution was concentrated in vacuo, and the residue taken up in ethyl acetate (200 mL) and washed with water (3×200 mL) and then sat. aq sodium chloride solution (150 mL) and dried over anhydrous Na_2SO_4 and concentrated to a pale-brown gum in vacuo. The residue was taken up in 1,4-dioxan (160 mL) and 2-amino-4-chlorothieno[2,3-*d*]pyrimidine-6-carboxylic acid ethyl ester (12.85 g, 50 mmol) and aq potassium phosphate (tribasic; 2.0 M; 40 mL) were added under a nitrogen atmosphere. Dichlorobis(triphenylphosphine)palladium(II) (cat.) was then added and the mixture heated at 100 °C (oil bath temperature) for 3 h. The mixture was allowed to cool and ethyl acetate (400 mL) added. This mixture was washed with sat. aq sodium chloride solution (100 mL), dried over anhydrous sodium sulfate, and concentrated to a pale-yellow solid, which was washed with diethyl ether/hexane (1:1) and then dried in vacuo at 40 °C to afford the title compound **26** (10.7 g, 45%) as an off-white solid: TLC $R_f = 0.13$ (EtOAc/hexane 1:3); LCMS $t_R = 2.79$ min; $m/z = 476$, 474 $[M + H]^+$. ^{1}H NMR (400 MHz; DMSO-d_6) δ 1.28 (t, 3H, $J = 7.1$ Hz), 4.29 (q, 2H, $J = 7.1$ Hz), 5.22 (s, 2H), 7.32−7.37 (m, 1H), 7.38−7.43 (m, 3H), 7.44−7.47 (m, 2H), 7.48 (s, 1H), 7.52 (brs, 2H), 7.84 (s, 1H).

2-Amino-4-(5-benzyloxy-2,4-dichlorophenyl)thieno[2,3-*d*]pyrimidine-6-carboxylic Acid Ethylamide (28). A suspension of 2-amino-4-(5-benzyloxy-2,4-dichlorophenyl)thieno[2,3-*d*]pyrimidine-6-carboxylic acid ethyl ester (**26**; 14.0 g, 29.5 mmol) in methanolic ethylamine (2.0 M; 400 mL) was heated at reflux for 18 h. The resulting solution was concentrated and the residue triturated with diethyl ether/hexane and then filtered and dried in vacuo at 60 °C to furnish the title compound **28** (11.8 g. 84%) as a pale-brown powder: LCMS $t_R = 2.65$ min; $m/z = 475.1$, 473. $[M + H]^+$. ^{1}H NMR (400 MHz; DMSO-d_6) δ 1.08 (t, 3H, $J = 7.1$ Hz), 3.23 (m, 2H), 5.23 (s, 2H), 7.24 (brs, 2H), 7.32−7.38 (m, 1H), 7.38−7.44 (m, 2H), 7.44−7.48 (m, 2H), 7.49 (s, 1H), 7.54 (s, 1H), 7.86 (s, 1H), 8.53 (brt, 1H, $J = 5.5$ Hz).

2-Amino-4-(2,4-dichloro-5-hydroxyphenyl)thieno[2,3-*d*]pyrimidine-6-carboxylic Acid Ethylamide (31). Boron trichloride solution (1.0 M in DCM, 100 mL, 0.10 mol) was added to a suspension of 2-amino-4-(5-benzyloxy-2,4-dichlorophenyl)thieno[2,3-*d*]pyrimidine-6-carboxylic acid ethylamide (**28**; 11.8 g, 24.9 mmol) in DCM at −78 °C under a nitrogen atmosphere. The suspension was stirred for 3 h at room temperature and then cooled in an ice/water bath. Methanol (20 mL) was added cautiously, and the resulting mixture was stirred for 1 h and then concentrated to a yellow/green solid. The solids were suspended in aq sodium acetate (10% w/v; 500 mL) and extracted with ethyl acetate (1000 mL). The extracts were washed with water (2×400 mL) and then sat. aq sodium chloride solution (200 mL). The organic solution was dried over anhydrous Na_2SO_4 and concentrated to a pale-brown solid in vacuo, which was washed with hexane, filtered, and dried in vacuo to afford the title compound **31** (8.3 g, 87%) as a pale-brown solid: LCMS $t_R = 2.18$ min; $m/z = 386$, 384 $[M + H]^+$. ^{1}H NMR (400 MHz; DMSO-d_6) δ 1.07 (t, 3H, $J = 7.4$ Hz), 3.21 (m, 2H), 7.05 (s, 1H), 7.26 (brs, 2H), 7.59 (s, 1H), 7.70 (s, 1H), 8.58 (brt, 1H, $J = 5.3$ Hz), 10.89 (s, 1H).

2-Amino-4-[2,4-dichloro-5-(2-diethylaminoethoxy)phenyl]thieno[2,3-*d*]pyrimidine-6-carboxylic Acid Ethylamide (34a).

Cesium carbonate (3.2 g, 10 mmol) was added to a stirred solution of 2-amino-4-(2,4-dichloro-5-hydroxyphenyl)thieno-[2,3-*d*]pyrimidine-6-carboxylic acid ethylamide (2.25 g, 5.9 mmol) in DMF (20 mL). 2-Bromo-*N*,*N*-diethylethylamine hydrobromide (Aldrich; 2.0 g, 7.7 mmol) was added and the mixture heated at 100 °C for 1 h. The resulting suspension was allowed to cool and concentrated to a brown solid. Dichloromethane (200 mL) was added to dissolve the crude solids and the organic solution then washed with water (4 × 200 mL), followed by sat. aq sodium chloride solution (1 × 200 mL). The phases were separated, and the organic phase was dried over anhydrous Na_2SO_4 and concentrated to a dark-brown gum, which solidified on standing. The crude product was purified by column chromatography on silica gel, eluting with dichloromethane/methanol (9:1) to give the product as a pale-brown gum. Trituration with diethyl ether/hexane (1:1), filtration, and drying in vacuo gave the title compound **34a** (1.7 g, 60%) as an off-white powder: TLC $R_f = 0.10$ (DCM/MeOH 9:1); LCMS $t_R = 1.86$ min; $m/z = 484$, 482 $[M + H]^+$. ^{1}H NMR (400 MHz; DMSO-d_6) δ 0.95 (t, 6H, $J = 7.1$ Hz), 1.07 (t, 3H, $J = 7.2$ Hz), 2.54 (q, 4H, $J = 7.1$ Hz), 2.80 (brt, 2H, $J = 5.5$ Hz), 3.21 (m, 2H), 4.12 (brt, 2H, $J = 5.5$ Hz), 7.27 (brs, 2H), 7.38 (s, 1H), 7.58 (s, 1H), 7.82 (s, 1H), 8.56 (brt, 1H, $J = 5.5$ Hz). ^{13}C NMR (100.6 MHz; DMSO-d_6) δ 12.0 (CH_3), 14.7 (CH_3), 34.0 (CH_2), 47.1 (CH_2), 50.9 (CH_2), 68.4 (CH_2), 115.3 (CH), 121.3 (C), 121.3 (CH), 122.3 (C), 123.0 (C), 130.3 (CH), 132.6 (C), 135.6 (C), 153.0 (C), 160.8 (C), 161.1 (C), 161.5 (C), 171.1 (C). HRMS calcd for $C_{21}H_{25}Cl_2N_5O_2S$ $[M + H]^+$ 482.1184, found 482.1196. HPLC (method A) 99.3% ($t_R = 4.68$ min).

2-Amino-4-[2,4-dichloro-5-(2,2-diethoxy−ethoxy)phenyl]thieno[2,3-*d*]pyrimidine-6-carboxylic Acid Ethylamide (35). Cesium carbonate (5.0 g, 15.3 mmol) was added to a solution of 2-amino-4-(2,4-dichloro-5-hydroxyphenyl)thieno[2,3-*d*]pyrimidine-6-carboxylic acid ethylamide (**31**, 3.85 g, 10.0 mmol) in DMF (20 mL). Bromoacetaldehyde diethyl acetal (1.8 mL, 12 mmol) was added, and the reaction mixture was heated to 125 °C for 4 h. The resulting suspension was allowed to cool to ambient temperature and water (300 mL) was added and the mixture extracted with DCM (2 × 100 mL). The combined organic extracts were washed with water (4 × 200 mL) and then sat. aq sodium chloride solution (200 mL), dried over anhydrous Na_2SO_4, and filtered. The filtrate solvents were removed in vacuo to afford a pale-brown solid. The crude product was purified by column chromatography on silica gel, eluting with EtOAc/hexane (2:3) to give the title compound **35** (3.58 g, 71%) as a pale-yellow solid: TLC $R_f = 0.20$ (EtOAc/hexane 1:1); LCMS $t_R = 2.61$ min; $m/z = 501$, 499 $[M + H]^+$. ^{1}H NMR (400 MHz, DMSO-d_6) δ 1.07 (t, 3H, $J = 7.1$ Hz), 1.13 (t, 6H, $J = 7.1$ Hz), 3.22 (m, 2H), 3.54−3.62 (m, 2H), 3.65−3.73 (m, 2H), 4.08 (d, 2H, $J = 5.3$ Hz), 4.84 (t, 1H, $J = 5.3$ Hz), 7.22 (brs, 2H), 7.43 (s, 1H), 7.57 (s, 1H), 7.81 (s, 1H), 8.53 (brt, 1H, $J = 5.6$ Hz).

General Procedure A: Preparation of 34j to 34m by Reductive Amination. Aqueous HCl (6 N, 0.5 mL) was added to a solution of **35** (200 mg, 0.40 mmol) in THF (2.5 mL), and the mixture was stirred at ambient temperature for ca. 48 h. DCM (10 mL) was added, followed by the appropriate amine (5 equiv), and the mixture was stirred for 15 min. Sodium triacetoxyborohydride (750 mg, 3.54 mmol) was added and the resulting suspension stirred for 1.5 h. Further DCM (10 mL) was added, followed by aq sodium hydroxide solution (2.0 M, 5 mL) and the mixture was stirred for 5 min. The phases were separated, and the organic phase solvents were removed in vacuo. The crude product was purified by preparative HPLC at pH 4.

2-Amino-4-[2,4-dichloro-5-(2-cyclohexyaminoethoxy)phenyl]thieno[2,3-*d*]pyrimidine-6-carboxylic Acid Ethylamide (34j). This compound was prepared using general procedure A from **35** (200 mg, 0.40 mmol) and cyclohexylamine to afford the title compound **34j** (formate salt) (28 mg, 12%) as an off-white solid: LCMS $t_R = 1.98$ min; $m/z = 510$, 508 $[M + H]^+$. ^{1}H NMR (400 MHz; DMSO-d_6) δ 1.00−1.10 (m, 3H), 1.08 (t, 3H, $J =$ 7.0 Hz), 1.13−1.25 (m, 2H), 1.50−1.58 (m, 1H), 1.62−1.71 (m, 2H), 1.82−1.90 (m, 2H), 2.59 (m, 1H), 3.03 (brt, 2H, $J = 5.6$ Hz), 3.22 (m, 2H), 4.19 (brt, 2H, $J = 5.6$ Hz), 7.27 (brs, 2H), 7.38 (s, 1H), 7.57 (s, 1H), 7.84 (s, 1H), 8.23 (s, 1H), 8.60 (brt, 1H, $J =$ 5.6 Hz). ^{13}C NMR (100.6 MHz; DMSO-d_6) δ 14.7 (CH_3), 24.3 (CH_2), 25.6 (CH_2), 32.0 (CH_2), 34.0 (CH_2), 44.1 (CH_2), 55.7 (CH), 68.9 (CH_2), 115.5 (CH), 121.2 (CH), 121.3 (C), 122.6 (C), 123.2 (C), 130.4 (CH), 132.6 (C), 135.6 (C), 152.8 (C), 160.8 (C), 161.1 (C), 161.5 (C), 164.1 (CH), 171.2 (C). HRMS calcd for $C_{23}H_{27}Cl_2N_5O_2S$ $[M + H]^+$ 508.1341, found 508.1355. HPLC (method A) 98.3% ($t_R = 4.98$ min).

2-Amino-4-{2,4-dichloro-5-[2-(4,4-difluoropiperidin-1-yl)ethoxy]phenyl}thieno[2,3-*d*]pyrimidine-6-carboxylic Acid Ethylamide (34m). This compound was prepared using general procedure A from **35** (200 mg, 0.40 mmol) and 4,4-difluoropiperidine hydrochloride (300 mg, 1.9 mmol) to afford the title compound **34m** (30 mg, 14%) as an off-white solid: LCMS $t_R = 2.01$ min; $m/z = 532$, 530 $[M + H]^+$. ^{1}H NMR (400 MHz; DMSO-d_6) δ 1.07 (t, 3H, $J = 7.2$ Hz), 1.86−1.97 (m, 4H), 2.64 (m, 4H), 2.82 (t, 2H, $J = 5.6$ Hz), 3.22 (m, 2H), 4.21 (t, 2H, $J = 5.6$ Hz), 7.22 (brs, 2H), 7.40 (s, 1H), 7.53 (s, 1H), 7.81 (s, 1H), 8.53 (brt, 1H, $J = 5.6$ Hz). ^{13}C NMR (100.6 MHz; DMSO-d_6) δ 14.7 (CH_3), 33.4 (CH_2, t, $J_{C-F} = 22$ Hz), 34.0 (CH_2), 49.7 (CH_2, t, $J_{C-F} = 5$ Hz), 55.1 (CH_2), 67.8 (CH_2), 115.4 (CH), 121.2 (CH), 121.3 (C), 122.5 (C), 122.6 (C, t, $J_{C-F} = 241$ Hz), 123.1 (C), 130.4 (CH), 132.6 (C), 135.6 (C), 152.9 (C), 160.8 (C), 161.1 (C), 161.5 (C), 171.1 (C). HRMS calcd for $C_{22}H_{23}Cl_2F_2N_5O_2S$ $[M + H]^+$ 530.0996, found 530.1003. HPLC (method A) 90.2% ($t_R = 5.09$ min).

2-Amino-4-[2,4-dichloro-5-(2-pyrrolidin-1-yl-ethoxy)phenyl]thieno[2,3-*d*]pyrimidine-6-carboxylic Acid Ethylamide (34d). This compound was made using the synthetic procedure described for **34a**. Thus 2-amino-4-(2,4-dichloro-5-hydroxy-phenyl)thieno[2,3-*d*]pyrimidine-6-carboxylic acid ethylamide (**31**, 150 mg, 0.39 mmol) was reacted with 1-(2-chloroethyl)-pyrrolidine hydrochloride (Aldrich; 79 mg, 0.47 mmol). The crude product was purified by column chromatography on silica gel, eluting with dichloromethane/methanol (9:1) to give the product as a yellow glass. Trituration with EtOAc/hexane (1:1), filtration, and drying in vacuo gave the title compound **34d** (89 mg, 48%) as a cream-colored solid: TLC $R_f = 0.14$ (DCM/MeOH 9:1); LCMS $t_R = 1.83$ min; $m/z = 482$, 480 $[M + H]^+$. ^{1}H NMR (400 MHz; DMSO-d_6) δ 1.07 (t, 3H, $J = 7.3$ Hz), 1.64−1.69 (m, 4H), 2.51−2.57 (m, 4H,), 2.82 (brt, 2H, $J = 5.5$ Hz) 3.22 (m, 2H), 4.19 (brt, 2H, $J = 5.5$ Hz), 7.24 (brs, 2H), 7.38 (s, 1H), 7.57 (s, 1H), 7.81 (s, 1H), 8.54 (brt, 1H, $J = 5.6$ Hz). ^{13}C NMR (100.6 MHz; DMSO-d_6) δ 14.7 (CH_3), 23.2 (CH_2), 34.0 (CH_2), 53.9 (CH_2), 54.1 (CH_2), 68.9 (CH_2), 115.3 (CH), 121.2 (CH), 121.3 (C), 122.3 (C), 123.0 (C), 130.4 (CH), 132.6 (C), 135.6 (C), 152.9 (C), 160.8 (C), 161.1 (C), 161.5 (C), 171.1 (C). HRMS, calcd for $C_{21}H_{23}Cl_2N_5O_2S$ $[M + H]^+$ 480.1028, found 480.1004. HPLC (method B) 99.9% ($t_R = 2.10$ min).

2-Amino-4-(5-benzyloxy-2,4-dichlorophenyl)thieno[2,3-*d*]pyrimidine-6-carboxylic Acid (27). Sodium hydroxide (pearlescent; 190 mg, 4.76 mmol) was added to 2-amino-4-(5-benzyloxy-2,4-dichlorophenyl)thieno[2,3-*d*]pyrimidine-6-carboxylic acid ethyl ester (**26**; 1.13 g, 2.38 mmol). Ethanol (25 mL) was added, followed by water (2.5 mL), and the resulting suspension was heated to reflux for 50 min, causing a brown solution to form after 10 min. The reaction mixture was allowed to cool and ethanol was removed in vacuo. Water (25 mL) was added to the residue, and the mixture was cooled with an ice water bath and neutralized by careful addition of conc HCl. The water was removed by freeze-drying to afford the title compound **27** (1.34 g, quant) as a finely divided yellow powder (including 2.0 equiv of NaCl): LCMS $t_R = 2.60$ min; $m/z = 448$, 446 $[M + H]^+$. ^{1}H NMR (400 MHz; DMSO-d_6) δ 5.21 (s, 2H), 7.13 (s, 1H), 7.22 (brs, 2H), 7.32−7.37 (m, 1H), 7.38−7.43 (m, 2H), 7.43−7.48 (m, 3H), 7.80 (s, 1H), CO_2H not observed.

2-Amino-4-(5-benzyloxy-2,4-dichlorophenyl)thieno[2,3-*d*]pyrimidine-6-carboxylic Acid Cyclopropylamide (29).

2-Amino-4-(5-benzyloxy-2,4-dichlorophenyl)thieno[2,3-*d*]pyrimidine-6-carboxylic acid·2NaCl (**27**) (1.34 g, 2.38 mmol) was dissolved in DMF (25 mL) and *O*-(7-azabenzotriazolo-1-yl)-*N*,*N*,*N*′,*N*′-tetramethyluroniumhexafluorophosphate (HATU; 1.176 g, 3.1 mmol) was added, followed by diisopropylethylamine (1.2 mL, 6.9 mmol) and then cyclopropylamine (0.24 mL, 3.46 mmol). The reaction mixture was heated to 50 °C (oil bath temperature) for 1 h. The mixture was cooled and DMF removed in vacuo. The residue was partitioned between water (250 mL) and EtOAc (250 mL), the phases were separated, and the organic phase was washed with water (200 mL) and then sat. aq NaCl (250 mL) and dried over Na_2SO_4. The mix was filtered and filtrate solvents removed in vacuo, and the resulting residue purified by flash chromatography on silica gel (50 g) eluting with a gradient of 25−75% EtOAc in hexane to afford the title compound **29** (1.14 g, 98%) as a light-brown solid: LCMS $t_R = 2.69$ min; $m/z = 487$, 485 $[M + H]^+$. ^{1}H NMR (400 MHz; DMSO-d_6) δ 0.49−0.54 (m, 2H), 0.65−0.70 (m, 2H), 2.76 (m, 1H), 5.22 (s, 2H), 7.29 (brs, 2H), 7.32−7.50 (m, 6H), 7.52 (s, 1H), 7.86 (s, 1H), 8.54 (d, 1H, $J = 3.8$ Hz).

2-Amino-4-(2,4-dichloro-5-hydroxyphenyl)thieno[2,3-*d*]pyrimidine-6-carboxylic Acid Cyclopropylamide (32). 2-Amino-4-(5-benzyloxy-2,4-dichlorophenyl)thieno[2,3-*d*]pyrimidine-6-carboxylic acid cyclopropylamide (**27**; 2.33 g, 4.80 mmol) was suspended in anhydrous DCM (50 mL) under a nitrogen atmosphere and cooled with dry ice/acetone bath (ca. −78 °C). Boron trichloride (1.0 M in dichloromethane, 26.3 mL, 26.3 mmol) was added and the reaction mixture stirred for 15 min. The cooling bath was removed and mixture was stirred for 18 h at ambient temperature. The reaction mixture was cooled with ice−water bath, and methanol (10 mL) was added dropwise. The mixture was stirred for 1 h, the solvents removed in vacuo, and the residual solid partitioned between EtOAc (100 mL) and sat. $NaHCO_3$ (aq) solution (100 mL). The phases were separated and the organic phase was washed with sat. NaCl solution (100 mL), dried over Na_2SO_4, filtered, and the filtrate removed in vacuo to afford the title compound **32** (1.37 g, 72%) as a pale-brown powder: LCMS $t_R = 2.21$ min; $m/z = 397$, 395 $[M + H]^+$. ^{1}H NMR (400 MHz; DMSO-d_6) δ 0.48−0.53 (m, 2H), 0.64−0.69 (m, 2H), 2.76 (m, 1H), 7.07 (s, 1H), 7.27 (brs, 2H), 7.57 (s, 1H), 7.71 (s, 1H), 8.57 (d, 1H, $J = 4.1$ Hz), 10.94 (brs, 1H).

2-Amino-4-[2,4-dichloro-5-(2-diethylaminoethoxy)phenyl]thieno[2,3-*d*]pyrimidine-6-carboxylic Acid Cyclopropylamide (34b). 2-Amino-4-(2,4-dichloro-5-hydroxyphenyl)thieno[2,3-*d*]pyrimidine-6-carboxylic acid cyclopropylamide (**32**; 0.854 g, 2.16 mmol was dissolved in anhydrous THF (50 mL). *N*,*N*-diethylethanolamine (0.34 mL, 2.59 mmol) was added, followed by triphenylphosphine (0.850 g, 3.24 mmol) and diisopropylazodicarboxylate (0.64 mL, 3.24 mmol). The reaction mixture was stirred at rt for 3 h and then EtOAc (200 mL) was added and the mixture washed sequentially with water (200 mL), sat. $NaHCO_3$ solution, and sat. NaCl solution. The organic phase was dried over Na_2SO_4, filtered, and the filtrate solvents removed in vacuo to afford a brown oil, which was purified by flash chromatography on silica gel (50 g) eluting with a gradient of 2−5% MeOH in DCM to afford the title compound **34b** (0.434 g, 41%) as a cream-colored solid: LCMS $t_R = 1.86$ min; $m/z = 496$, 494 $[M + H]^+$. ^{1}H NMR (400 MHz; DMSO-d_6) δ 0.48−0.52 (m, 2H), 0.64−0.69 (m, 2H), 0.96 (t, 6H, $J = 7.1$ Hz), 2.49−2.57 (brm, 4H), 2.75 (m, 1H), 2.80 (brm, 2H), 4.11 (brt, 2H, $J = 5.5$ Hz), 7.26 (brs, 2H), 7.37 (s, 1H), 7.56 (s, 1H), 7.81 (s, 1H), 8.54 (d, 1H, $J = 3.9$ Hz). ^{13}C NMR (100.6 MHz; DMSO-d_6) δ 5.7 (CH_2), 12.0 (CH_3), 22.9 (CH), 47.1 (CH_2), 50.9 (CH_2), 68.4 (CH_2), 115.3 (CH), 121.3 (C), 121.5 (CH), 122.3 (C), 123.0 (C), 130.3 (CH), 132.3 (C), 135.6 (C), 153.0 (C), 161.1 (C), 161.6 (C), 162.3 (C), 171.2 (C). HRMS calcd for $C_{22}H_{25}Cl_2N_5O_2S$ $[M + H]^+$ 494.1184, found 494.1169. HPLC (method B) 98.8% ($t_R = 2.47$ min).

2-Amino-4-[2,4-dichloro-5-(1-ethyl-pyrrolidin-3-yloxy)phenyl]thieno[2,3-*d*]pyrimidine-6-carboxylic Acid Ethylamide (34i). 2-Amino-4-(2,4-dichloro-5-hydroxyphenyl)thieno[2,3-*d*]pyrimidine-6-carboxylic acid ethylamide (**31**; 0.700 g, 1.83 mmol) was dissolved in anhydrous THF (50 mL). 1-Ethyl-3-pyrrolidinol (0.26 mL, 2.18 mmol) was added, followed by triphenylphosphine (0.863 g, 3.29 mmol) and diisopropylazodicarboxylate (0.65 mL, 3.29 mmol). The reaction mixture was stirred at rt for 16 h and then EtOAc (200 mL) was added and the mixture washed sequentially with water (200 mL), sat. $NaHCO_3$ solution (100 mL), and sat. NaCl solution (100 mL). The organic phase was dried over Na_2SO_4, filtered, and the filtrate solvents removed in vacuo to afford a brown oil, which was purified by flash chromatography on silica gel (50 g) eluting with 10% MeOH in DCM to afford the title compound **34i** (0.359 g, 41%) as a cream-colored powder: LCMS $t_R = 1.83$ min; $m/z = 482$, 480 $[M + H]^+$. ^{1}H NMR (400 MHz; DMSO-d_6) δ 1.01 (t, 3H, $J = 7.4$ Hz), 1.07 (t, 3H, $J = 7.4$ Hz), 1.81 (m, 1H), 2.20−2.47 (m, 4H), 2.65−2.80 (m, 3H), 3.20 (m, 2H), 4.96 (m, 1H), 7.27 (s, 1H), 7.27 (brs, 2H), 7.56 (s, 1H), 7.82 (s, 1H), 8.55 (brt, 1H, $J = 5.6$ Hz). ^{13}C NMR (100.6 MHz; DMSO-d_6) δ 13.6 (CH_3), 14.7 (CH_3), 31.6 (CH_2), 34.0 (CH_2), 49.2 (CH_2), 52.0 (CH_2), 59.3 (CH_2), 78.2 (CH), 115.9 (CH), 121.2 (CH), 121.3 (C), 122.3 (C), 123.5 (C), 130.6 (CH), 132.6 (C), 135.5 (C), 152.0 (C), 160.8 (C), 161.1 (C), 161.5 (C), 171.1 (C). HRMS calcd for $C_{21}H_{23}Cl_2N_5O_2S$ $[M + H]^+$ 480.1028, found 480.1017. HPLC (method B) 99.1% ($t_R = 2.43$ min).

Acknowledgment. We are grateful to Tim Haymes for analytical support, to Adam Hold and Loic Le Strat for compound purification, to Ruth Botting, Sarah Denny, Kiri Tan, Lynne Barratt, Eamon McCay, Jason Busby, Vanessa Martins, and Alan Henley for DMPK and bioanalysis studies, and to Sharon Gowan and Alexis de Haven Brandon for tumour xenograft and biomarker studies. We are also grateful to Helen Browne for assistance with manuscript preparation. This work was supported by Cancer Research UK [CRUK] programme grant numbers CA309/A2187 and C309/A8274. The ICR acknowledges NHS funding to the NIHR Biomedical Research Centre and from Vernalis. Paul Workman is a Cancer Research UK Life Fellow. The authors from The Institute of Cancer Research (ICR) declare a conflict of interest. The ICR has a commercial interest in Hsp90 inhibitors and operates a rewards to inventors scheme.

Supporting Information Available: Data relating to the PC3 human prostate cancer xenograft model for compound **34a**; experimental procedures for the FP assay and synthesis of the FP assay probe and methods and parameters relating to X-ray crystallography and protein production; full chemistry experimental procedures and characterization data; methods for analytical and preparative HPLC; commercial sources for fragment and in silico screening hits; protocols relating to the 1D NMR screening of fragments; description of the process applied for the in silico screening campaign. This material is available free of charge via the Internet at http://pubs.acs.org.

References

(1) Mosser, D. D.; Morimoto, R. I. Molecular chaperones and the stress of oncogenesis. *Oncogene* **2004**, *23*, 2907–2918.
(2) Pearl, L. H.; Prodromou, C. Structure and mechanism of the hsp90 molecular chaperone machinery. *Annu. Rev. Biochem.* **2006**, *75*, 271–294.
(3) Obermann, W. M.; Sondermann, H.; Russo, A. A.; Pavletich, N. P.; Hartl, F. U. In vivo function of Hsp90 is dependent on ATP binding and ATP hydrolysis. *J. Cell Biol.* **1998**, *143*, 901–910.
(4) Panaretou, B.; Prodromou, C.; Roe, S. M.; O'Brien, R.; Ladbury, J. E.; Piper, P. W.; Pearl, L. H. ATP binding and hydrolysis are essential to the function of the Hsp90 molecular chaperone in vivo. *EMBO J.* **1998**, *17*, 4829–4836.
(5) Pearl, L. H.; Prodromou, C.; Workman, P. The Hsp90 molecular chaperone: an open and shut case for treatment. *Biochem. J.* **2008**, *410*, 439–453.

(6) For a list, see the web page maintained by D. Picard: http://www.picard.ch/downloads/Hsp90interactors.pdf. Accessed on July 13, 2009
(7) Whitesell, L.; Lindquist, S. L. HSP90 and the chaperoning of cancer. *Nat. Rev. Cancer* **2005**, *5*, 761–772.
(8) Maloney, A.; Workman, P. HSP90 as a new therapeutic target for cancer therapy: the story unfolds. *Expert Opin. Biol. Ther.* **2002**, *2*, 3–24.
(9) Kamal, A.; Boehm, M. F.; Burrows, F. J. Therapeutic and diagnostic implications of Hsp90 activation. *Trends Mol. Med.* **2004**, *10*, 283–290.
(10) Chiosis, G.; Vilenchik, M.; Kim, J.; Solit, D. Hsp90: the vulnerable chaperone. *Drug Discovery Today* **2004**, *9*, 881–888.
(11) Hanahan, D.; Weinberg, R. A. The hallmarks of cancer. *Cell* **2000**, *100*, 57–70.
(12) Workman, P. Combinatorial attack on multistep oncogenesis by inhibiting the Hsp90 molecular chaperone. *Cancer Lett.* **2004**, *206*, 149–157.
(13) DeBoer, C.; Meulman, P. A.; Wnuk, R. J.; Peterson, D. H. Geldanamycin, a new antibiotic. *J. Antibiot. (Tokyo)* **1970**, *23*, 442–447.
(14) Supko, J. G.; Hickman, R. L.; Grever, M. R.; Malspeis, L. Preclinical pharmacologic evaluation of geldanamycin as an antitumor agent. *Cancer Chemother. Pharmacol.* **1995**, *36*, 305–315.
(15) Neckers, L.; Schulte, T. W.; Mimnaugh, E. Geldanamycin as a potential anticancer agent: its molecular target and biochemical activity. *Invest. New Drugs* **1999**, *17*, 361–373.
(16) Delmotte, P.; Delmotte-Plaque, J. A new antifungal substance of fungal origin. *Nature* **1953**, *171*, 344.
(17) Soga, S.; Shiotsu, Y.; Akinaga, S.; Sharma, S. V. Development of radicicol analogues. *Curr. Cancer Drug Targets* **2003**, *3*, 359–369.
(18) Roe, S. M.; Prodromou, C.; O'Brien, R.; Ladbury, J. E.; Piper, P. W.; Pearl, L. H. Structural basis for inhibition of the Hsp90 molecular chaperone by the antitumor antibiotics radicicol and geldanamycin. *J. Med. Chem.* **1999**, *42*, 260–266.
(19) Hostein, I.; Robertson, D.; DiStefano, F.; Workman, P.; Clarke, P. A. Inhibition of signal transduction by the Hsp90 inhibitor 17-allylamino-17-demethoxygeldanamycin results in cytostasis and apoptosis. *Cancer Res.* **2001**, *61*, 4003–4009.
(20) Schulte, T. W.; Neckers, L. M. The benzoquinone ansamycin 17-allylamino-17-demethoxygeldanamycin binds to HSP90 and shares important biologic activities with geldanamycin. *Cancer Chemother. Pharmacol.* **1998**, *42*, 273–279.
(21) Banerji, U.; O'Donnell, A.; Scurr, M.; Pacey, S.; Stapleton, S.; Asad, Y.; Simmons, L.; Maloney, A.; Raynaud, F.; Campbell, M.; Walton, M.; Lakhani, S.; Kaye, S.; Workman, P.; Judson, I. Phase I pharmacokinetic and pharmacodynamic study of 17-allylamino, 17-demethoxygeldanamycin in patients with advanced malignancies. *J. Clin. Oncol.* **2005**, *23*, 4152–4161.
(22) Goetz, M. P.; Toft, D.; Reid, J.; Ames, M.; Stensgard, B.; Safgren, S.; Adjei, A. A.; Sloan, J.; Atherton, P.; Vasile, V.; Salazaar, S.; Adjei, A.; Croghan, G.; Erlichman, C. Phase I trial of 17-allylamino-17-demethoxygeldanamycin in patients with advanced cancer. *J. Clin. Oncol.* **2005**, *23*, 1078–1087.
(23) Weigel, B. J.; Blaney, S. M.; Reid, J. M.; Safgren, S. L.; Bagatell, R.; Kersey, J.; Neglia, J. P.; Ivy, S. P.; Ingle, A. M.; Whitesell, L.; Gilbertson, R. J.; Krailo, M.; Ames, M.; Adamson, P. C. A Phase I Study of 17-Allylaminogeldanamycin in Relapsed/Refractory Pediatric Patients with Solid Tumors: A Children's Oncology Group Study. *Clin. Cancer Res.* **2007**, *13*, 1789–1793.
(24) Solit, D. B.; Osman, I.; Polsky, D.; Panageas, K. S.; Daud, A.; Goydos, J. S.; Teitcher, J.; Wolchok, J. D.; Germino, F. J.; Krown, S. E.; Coit, D.; Rosen, N.; Chapman, P. B. Phase II Trial of 17-Allylamino-17-Demethoxygeldanamycin in Patients with Metastatic Melanoma. *Clin. Cancer Res.* **2008**, *14*, 8302–8307.
(25) Kamal, A.; Thao, L.; Sensintaffar, J.; Zhang, L.; Boehm, M. F.; Fritz, L. C.; Burrows, F. J. A high-affinity conformation of Hsp90 confers tumour selectivity on Hsp90 inhibitors. *Nature* **2003**, *425*, 407–410.
(26) da Rocha, D. S.; Friedlos, F.; Light, Y.; Springer, C.; Workman, P.; Marais, R. Activated B-RAF is an Hsp90 client protein that is targeted by the anticancer drug 17-allylamino-17-demethoxygeldanamycin. *Cancer Res.* **2005**, *65*, 10686–10691.
(27) Workman, P.; Burrows, F.; Neckers, L. Drugging the cancer chaperone HSP90: combinatorial therapeutic exploitation of oncogene addiction and tumor stress. *Ann. N.Y. Acad. Sci.* **2007**, *1113*, 202–216.
(28) Egorin, M. J.; Rosen, D. M.; Wolff, J. H.; Callery, P. S.; Musser, S. M.; Eiseman, J. L. Metabolism of 17-(allylamino)-17-demethoxygeldanamycin (NSC 330507) by murine and human hepatic preparations. *Cancer Res.* **1998**, *58*, 2385–2396.
(29) Kelland, L. R.; Sharp, S. Y.; Rogers, P. M.; Myers, T. G.; Workman, P. DT-Diaphorase expression and tumor cell sensitivity to 17-allylamino, 17-demethoxygeldanamycin, an inhibitor of heat shock protein 90. *J. Natl. Cancer Inst.* **1999**, *91*, 1940–1949.
(30) Meli, M.; Pennati, M.; Curto, M.; Daidone, M. G.; Plescia, J.; Toba, S.; Altieri, D. C.; Zaffaroni, N.; Colombo, G. Small-Molecule Targeting of Heat Shock Protein 90 Chaperone Function: Rational Identification of a New Anticancer Lead. *J. Med. Chem.* **2006**, *49*, 7721–7730.
(31) Gaspar, N.; Sharp, S. Y.; Pacey, S.; Jones, D.; Walton, M.; Vassal, G.; Eccles, S.; Pearson, A.; Workman, P. Acquired Resistance to 17-Allylamino-17-Demethoxygeldanamycin (Tanespimycin) in Glioblastoma Cells. *Cancer Res.* **2009**, *69*, 1966–1975.
(32) Kaur, G.; Belotti, D.; Burger, A. M.; Fisher-Nielson, K.; Borsotti, P.; Riccardi, E.; Thillainathan, J.; Hollingshead, M.; Sausville, E. A.; Giavazzi, R. Antiangiogenic properties of 17-(dimethylaminoethylamino)-17-demethoxygeldanamycin: an orally bioavailable heat shock protein 90 modulator. *Clin. Cancer Res.* **2004**, *10*, 4813–4821.
(33) Ge, J.; Normant, E.; Porter, J. R.; Ali, J. A.; Dembski, M. S.; Gao, Y.; Georges, A. T.; Grenier, L.; Pak, R. H.; Patterson, J.; Sydor, J. R.; Tibbitts, T. T.; Tong, J. K.; Adams, J.; Palombella, V. J. Design, synthesis, and biological evaluation of hydroquinone derivatives of 17-amino-17-demethoxygeldanamycin as potent, water-soluble inhibitors of Hsp90. *J. Med. Chem.* **2006**, *49*, 4606–4615.
(34) Sydor, J. R.; Normant, E.; Pien, C. S.; Porter, J. R.; Ge, J.; Grenier, L.; Pak, R. H.; Ali, J. A.; Dembski, M. S.; Hudak, J.; Patterson, J.; Penders, C.; Pink, M.; Read, M. A.; Sang, J.; Woodward, C.; Zhang, Y.; Grayzel, D. S.; Wright, J.; Barrett, J. A.; Palombella, V. J.; Adams, J.; Tong, J. K. Development of 17-allylamino-17-demethoxygeldanamycin hydroquinone hydrochloride (IPI-504), an anticancer agent directed against Hsp90. *Proc. Natl. Acad. Sci. U.S.A.* **2006**, *103*, 17408–17413.
(35) Modi, S.; Stopeck, A. T.; Gordon, M. S.; Mendelson, D.; Solit, D. B.; Bagatell, R.; Ma, W.; Wheler, J.; Rosen, N.; Norton, L.; Cropp, G. F.; Johnson, R. G.; Hannah, A. L.; Hudis, C. A. Combination of trastuzumab and tanespimycin (17-AAG, KOS-953) is safe and active in trastuzumab-refractory HER-2-overexpressing breast cancer: a phase I dose-escalation study. *J. Clin. Oncol.* **2007**, *25*, 5410–5417.
(36) Drysdale, M. J.; Brough, P. A. Medicinal chemistry of Hsp90 inhibitors. *Curr. Top. Med. Chem.* **2008**, *8*, 859–868.
(37) Chiosis, G. Discovery and development of purine-scaffold Hsp90 inhibitors. *Curr. Top. Med. Chem.* **2006**, *6*, 1183–1191.
(38) Chiosis, G.; Rodina, A.; Moulick, K. Emerging Hsp90 inhibitors: from discovery to clinic. *Anticancer Agents Med. Chem.* **2006**, *6*, 1–8.
(39) Chiosis, G.; Lopes, E. C.; Solit, D. Heat shock protein-90 inhibitors: a chronicle from geldanamycin to today's agents. *Curr. Opin. Invest. Drugs (Thomson Scientific)* **2006**, *7*, 534–541.
(40) Dymock, B. W.; Drysdale, M. J.; McDonald, E.; Workman, P. Inhibitors of HSP90 and other chaperones for the treatment of cancer. *Expert Opin. Ther. Pat.* **2004**, *14*, 837–847.
(41) Neckers, L.; Neckers, K. Heat-shock protein 90 inhibitors as novel cancer chemotherapeutics—an update. *Expert Opin. Emerging Drugs* **2005**, *10*, 137–149.
(42) Janin, Y. L. Heat shock protein 90 inhibitors. A text book example of medicinal chemistry?. *J. Med. Chem.* **2005**, *48*, 7503–7512.
(43) Drysdale, M. J.; Brough, P. A.; Massey, A.; Jensen, M. R.; Schoepfer, J. Targeting Hsp90 for the treatment of cancer. *Curr. Opin. Drug Discovery Dev.* **2006**, *9*, 483–495.
(44) McDonald, E.; Workman, P.; Jones, K. Inhibitors of the HSP90 molecular chaperone: attacking the master regulator in cancer. *Curr. Top. Med. Chem.* **2006**, *6*, 1091–1107.
(45) Messaoudi, S.; Peyrat, J. F.; Brion, J. D.; Alami, M. Recent advances in Hsp90 inhibitors as antitumor agents. *Anti-Cancer Agents Med. Chem.* **2008**, *8*, 761–782.
(46) Taldone, T.; Gozman, A.; Maharaj, R.; Chiosis, G. Targeting Hsp90: small-molecule inhibitors and their clinical development. *Curr. Opin. Pharmacol.* **2008**, *8*, 370–374.
(47) Taldone, T.; Sun, W.; Chiosis, G. Discovery and development of heat shock protein 90 inhibitors. *Bioorg. Med. Chem.* **2009**, *17*, 2225–2235.
(48) Kasibhatla, S. R.; Hong, K.; Biamonte, M. A.; Busch, D. J.; Karjian, P. L.; Sensintaffar, J. L.; Kamal, A.; Lough, R. E.; Brekken, J.; Lundgren, K.; Grecko, R.; Timony, G. A.; Ran, Y.; Mansfield, R.; Fritz, L. C.; Ulm, E.; Burrows, F. J.; Boehm, M. F. Rationally designed high-affinity 2-amino-6-halopurine heat shock protein 90 inhibitors that exhibit potent antitumor activity. *J. Med. Chem.* **2007**, *50*, 2767–2778.
(49) Lundgren, K.; Zhang, H.; Brekken, J.; Huser, N.; Powell, R. E.; Timple, N.; Busch, D. J.; Neely, L.; Sensintaffar, J. L.; Yang, Y. C.; McKenzie, A.; Friedman, J.; Scannevin, R.; Kamal, A.; Hong, K.; Kasibhatla, S. R.; Boehm, M. F.; Burrows, F. J. BIIB021, an orally

available, fully synthetic small-molecule inhibitor of the heat shock protein Hsp90. *Mol. Cancer Ther*. **2009**, *8*, 921–929.
(50) (a) Chandarlapaty, S.; Sawai, A.; Ye, Q.; Scott, A.; Silinski, M.; Huang, K.; Fadden, P.; Partdrige, J.; Hall, S.; Steed, P.; Norton, L.; Rosen, N.; Solit, D. B. SNX2112, a Synthetic Heat Shock Protein 90 Inhibitor, Has Potent Antitumor Activity against HER Kinase-Dependent Cancers. *Clin. Cancer Res*. **2008**, *14*, 240–248. (b) Huang, K. H.; Veal, J. M.; Fadden, R. P.; Rice, J. W.; Eaves, J.; Strachan, J. P.; Barabasz, A. F.; Foley, B. E.; Barta, T. E.; Ma, W.; Silinski, M. A.; Hu, M.; Partridge, J. M.; Scott, A.; Dubois, L. G.; Freed, T.; Steed, P. M.; Ommen, A. J.; Smith, E. D.; Hughes, P. F.; Woodward, A. R.; Hanson, G. J.; McCall, W. S.; Markworth, C. J.; Hinkley, L.; Jenks, M.; Geng, L.; Lewis, M.; Otto, J.; Pronk, B.; Verleysen, K.; Hall, S. E. Discovery of Novel 2-Aminobenzamide Inhibitors of Heat Shock Protein 90 as Potent, Selective and Orally Active Antitumor Agents. *J. Med. Chem*. **2009**, *52*, 4288–4305.
(51) Brough, P. A.; Aherne, W.; Barril, X.; Borgognoni, J.; Boxall, K.; Cansfield, J. E.; Cheung, K. M.; Collins, I.; Davies, N. G.; Drysdale, M. J.; Dymock, B.; Eccles, S. A.; Finch, H.; Fink, A.; Hayes, A.; Howes, R.; Hubbard, R. E.; James, K.; Jordan, A. M.; Lockie, A.; Martins, V.; Massey, A.; Matthews, T. P.; McDonald, E.; Northfield, C. J.; Pearl, L. H.; Prodromou, C.; Ray, S.; Raynaud, F. I.; Roughley, S. D.; Sharp, S. Y.; Surgenor, A.; Walmsley, D. L.; Webb, P.; Wood, M.; Workman, P.; Wright, L. 4,5-Diarylisoxazole Hsp90 chaperone inhibitors: potential therapeutic agents for the treatment of cancer. *J. Med. Chem*. **2008**, *51*, 196–218.
(52) Eccles, S. A.; Massey, A.; Raynaud, F. I.; Sharp, S. Y.; Box, G.; Valenti, M.; Patterson, L.; Haven Brandon, A.; Gowan, S.; Boxall, F.; Aherne, W.; Rowlands, M.; Hayes, A.; Martins, V.; Urban, F.; Boxall, K.; Prodromou, C.; Pearl, L.; James, K.; Matthews, T. P.; Cheung, K. M.; Kalusa, A.; Jones, K.; McDonald, E.; Barril, X.; Brough, P. A.; Cansfield, J. E.; Dymock, B.; Drysdale, M. J.; Finch, H.; Howes, R.; Hubbard, R. E.; Surgenor, A.; Webb, P.; Wood, M.; Wright, L.; Workman, P. NVP-AUY922: A Novel Heat Shock Protein 90 Inhibitor Active against Xenograft Tumor Growth, Angiogenesis, and Metastasis. *Cancer Res*. **2008**, *68*, 2850–2860.
(53) See www.clinicaltrials.gov for details of clinical trials relating Hsp90 inhibitors. Accessed on July 13, 2009.
(54) Congreve, M.; Chessari, G.; Tisi, D.; Woodhead, A. J. Recent developments in fragment-based drug discovery. *J. Med. Chem*. **2008**, *51*, 3661–3680.
(55) Erlanson, D. A. Fragment-based lead discovery: a chemical update. *Curr. Opin. Biotechnol*. **2006**, *17*, 643–652.
(56) Hajduk, P. J.; Greer, J. A decade of fragment-based drug design: strategic advances and lessons learned. *Nat. Rev. Drug Discovery* **2007**, *6*, 211–219.
(57) Hubbard, R. E. Fragment approaches in structure-based drug discovery. *J. Synchrotron Radiat*. **2008**, *15*, 227–230.
(58) Jahnke, W. Erlanson, D. A. Fragment-Based Approaches in Drug Discovery; Wiley: Weinheim, Germany, 2007.
(59) Jhoti, H. Leach, A. R. Structure-Based Drug Discovery; Springer: Dordrecht, The Netherlands, 2007.
(60) Hubbard, R. E.; Davis, B.; Chen, I.; Drysdale, M. J. The SeeDs approach: integrating fragments into drug discovery. *Curr. Top. Med. Chem*. **2007**, *7*, 1568–1581.
(61) Chiosis, G.; Timaul, M. N.; Lucas, B.; Munster, P. N.; Zheng, F. F.; Sepp-Lorenzino, L.; Rosen, N. A small molecule designed to bind to the adenine nucleotide pocket of Hsp90 causes Her2 degradation and the growth arrest and differentiation of breast cancer cells. *Chem. Biol*. **2001**, *8*, 289–299.
(62) Lepre, C. A.; Moore, J. M.; Peng, J. W. Theory and applications of NMR-based screening in pharmaceutical research. *Chem. Rev*. **2004**, *104*, 3641–3676.
(63) Mayer, M.; Meyer, B. Characterisation of ligand binding by saturation transfer difference NMR spectroscopy. *Angew. Chem., Int. Ed*. **1999**, *38*, 1784–1788.
(64) Dalvit, C.; Pevarello, P.; Tato, M.; Veronesi, M.; Vulpetti, A.; Sundstrom, M. Identification of compounds with binding affinity to proteins via magnetization transfer from bulk water. *J. Biomol. NMR* **2000**, *18*, 65–68.
(65) Hajduk, P. J.; Olejniczak, E. T.; Fesik, S. W. One-Dimensional Relaxation and Diffusion-Edited NMR Methods for Screening Compounds that Bind to Macromolecules. *J. Am. Chem. Soc*. **1997**, *119*, 12257–12261.
(66) Baurin, N.; Aboul-Ela, F.; Barril, X.; Davis, B.; Drysdale, M.; Dymock, B.; Finch, H.; Fromont, C.; Richardson, C.; Simmonite, H.; Hubbard, R. E. Design and characterization of libraries of molecular fragments for use in NMR screening against protein targets. *J. Chem. Inf. Comput. Sci*. **2004**, *44*, 2157–2166.
(67) Huth, J. R.; Park, C.; Petros, A. M.; Kunzer, A. R.; Wendt, M. D.; Wang, X.; Lynch, C. L.; Mack, J. C.; Swift, K. M.; Judge, R. A.; Chen, J.; Richardson, P. L.; Jin, S.; Tahir, S. K.; Matayoshi, E. D.; Dorwin, S. A.; Ladror, U. S.; Severin, J. M.; Walter, K. A.; Bartley, D. M.; Fesik, S. W.; Elmore, S. W.; Hajduk, P. J. Discovery and design of novel HSP90 inhibitors using multiple fragment-based design strategies. *Chem. Biol. Drug Des*. **2007**, *70*, 1–12.
(68) Barker, J. J.; Barker, O.; Boggio, R.; Chauhan, V.; Cheng, R. K.; Corden, V.; Courtney, S. M.; Edwards, N.; Falke, V. M.; Fusar, F.; Gardiner, M.; Hamelin, E. M.; Hesterkamp, T.; Ichihara, O.; Jones, R. S.; Mather, O.; Mercurio, C.; Minucci, S.; Montalbetti, C. A.; Muller, A.; Patel, D.; Phillips, B. G.; Varessi, M.; Whittaker, M.; Winkler, D.; Yarnold, C. J. Fragment-Based Identification of Hsp90 Inhibitors. *ChemMedChem* **2009**, *4*, 963–966.
(69) Barril, X.; Brough, P.; Drysdale, M.; Hubbard, R. E.; Massey, A.; Surgenor, A.; Wright, L. Structure-based discovery of a new class of Hsp90 inhibitors. *Bioorg. Med. Chem. Lett*. **2005**, *15*, 5187–5191.
(70) Knox, A. J. S.; Price, T.; Pawlak, M.; Golfis, G.; Flood, C. T.; Fayne, D.; Williams, D. C.; Meegan, M. J.; Lloyd, D. G. Integration of Ligand and Structure-Based Virtual Screening for the Identification of the First Dual Targeting Agent for Heat Shock Protein 90 (Hsp90) and Tubulin. *J. Med. Chem*. **2009**, *52*, 2177–2180.
(71) Barril, X.; Hubbard, R. E.; Morley, S. D. Virtual screening in structure-based drug discovery. *Mini. Rev. Med. Chem*. **2004**, *4*, 779–791.
(72) Wright, L.; Barril, X.; Dymock, B.; Sheridan, L.; Surgenor, A.; Beswick, M.; Drysdale, M.; Collier, A.; Massey, A.; Davies, N.; Fink, A.; Fromont, C.; Aherne, W.; Boxall, K.; Sharp, S.; Workman, P.; Hubbard, R. E. Structure−activity relationships in purine-based inhibitor binding to HSP90 isoforms. *Chem. Biol*. **2004**, *11*, 775–785.
(73) Baurin, N.; Baker, R.; Richardson, C.; Chen, I.; Foloppe, N.; Potter, A.; Jordan, A.; Roughley, S.; Parratt, M.; Greaney, P.; Morley, D.; Hubbard, R. E. Drug-like annotation and duplicate analysis of a 23-supplier chemical database totalling 2.7 million compounds. *J. Chem. Inf. Comput. Sci*. **2004**, *44*, 643–651.
(74) Howes, R.; Barril, X.; Dymock, B. W.; Grant, K.; Northfield, C. J.; Robertson, A. G.; Surgenor, A.; Wayne, J.; Wright, L.; James, K.; Matthews, T.; Cheung, K. M.; McDonald, E.; Workman, P.; Drysdale, M. J. A fluorescence polarization assay for inhibitors of Hsp90. *Anal. Biochem*. **2006**, *350*, 202–213.
(75) Wittenbrook, L. S. Chemistry of *N*-cyanodithioimidocarbonic acid. III. Intermediate in heterocyclic synthesis. *J. Heterocycl. Chem*. **1975**, *12*, 37–42.
(76) Clark, J.; Shahhet, M. S. Synthesis of thieno[2,3-*d*]pyrimidines from 4,6-dichloropyrimidine-5-carboxaldehydes. *J. Heterocycl. Chem*. **1993**, *30*, 1065–1072.
(77) Miyaura, N.; Suzuki, H. Palladium-Catalyzed Cross-Coupling Reactions of Organoboron Compounds. *Chem. Rev*. **2005**, *95*, 2457–2483.
(78) Zhu, L.; Duquette, J.; Zhang, M. An Improved Preparation of Arylboronates: Application in One-Pot Suzuki Biaryl Synthesis. *J. Org. Chem*. **2003**, *68*, 3729–3732.
(79) Hughes, D. L. The Mitsunobu Reaction. *Org. React*. **1992**, *42*, 335–656.
(80) PDB codes: compound **10** (cocrystal) = 2WI2, **10** (soak) = 2WI3, **11** = 2WI1, **12** = 2WI4, **13** = 2WI5, **21e** = 2WI6, and **34d** = 2WI7.
(81) (a) Dymock, B. W.; Drysdale, M. J.; Fromont, C.; Jordan, A.; Barril-Alonso, X. Preparation of pyrimidothiophenes as HSP90 inhibitors. PCT Int. Appl. WO200500521552, 2005. (b) Brough, P. A.; Barril-Alonso, X.; Drysdale, M. J. Preparation of pyrimidithiophene derivatives for use as HSP90 inhibitors. PCT International Application WO2006090094, 2006.
(82) Workman, P.; Twentyman, P.; Balkwill, F.; Balmain, A.; Chaplin, C.; Double, J. United Kingdom Coordinating Committee on Cancer Research guidelines for the welfare of animals in experimental neoplasia, 2nd Ed. *Br. J. Cancer* **1998**, *77*, 1–10.